

Review

A Review of Non-Soil Biochar Applications

Mattia Bartoli ¹, Mauro Giorcelli ¹, Pravin Jagdale ², Massimo Rovere ¹ and Alberto Tagliaferro ^{1,3,*}

¹ Department of Applied Science and Technology, Polytechnic of Turin, C.so Duca degli Abruzzi 24, 10129 Turin, Italy; mattia.bartoli@polito.it (M.B.); mauro.giorcelli@polito.it (M.G.); massimo.rovere@polito.it (M.R.)

² Center for Sustainable Future, Italian Institute of Technology, Via Livorno 60, 10144 Turin, Italy; pravin.jagdale@iit.it

³ Faculty of Science, University of Ontario Institute of Technology, 2000 Simcoe Street North, Oshawa, ON L1G 0C5, Canada

* Correspondence: alberto.tagliaferro@polito.it; Tel.: +39-011-097348

Received: 2 December 2019; Accepted: 5 January 2020; Published: 7 January 2020



Abstract: Biochar is the solid residue that is recovered after the thermal cracking of biomasses in an oxygen-free atmosphere. Biochar has been used for many years as a soil amendment and in general soil applications. Nonetheless, biochar is far more than a mere soil amendment. In this review, we report all the non-soil applications of biochar including environmental remediation, energy storage, composites, and catalyst production. We provide a general overview of the recent uses of biochar in material science, thus presenting this cheap and waste-derived material as a high value-added and carbonaceous source.

Keywords: biochar; environmental remediation; energy storage; composites; carbon

1. Introduction

The use of carbonaceous material is one of the most established practices in material science [1]. Nowadays, carbon fibers are used in so many commodities that they have become an unavoidable asset for the global market [2]. Together with carbon fibers, carbon black leads the global carbon revenue due to its use in the production of tires [3]. Over the years, highly costly carbon materials such as carbon nanotubes and graphene have fed the dreams of the scientific community with their astonishing conductive, optical, and mechanical properties [4,5]. Despite the expected revolution, these materials did not develop from research and small productions. In 2009, Segal et al. [6] said that the world was ready for the ton-scale production of graphene, but, in 2020, single layer graphene is still sold at 230 €/cm² and graphene oxide costs 140,000 €/kg [7]. In contrast, carbon black is sold for 1.5–0.95 €/kg [8]. High-tech carbon materials (i.e., carbon nanotubes, graphene and graphene oxide) have not yet fulfilled the promise of the new carbon era. While the world waits for the large scale commercialization of cheap pure carbon allotropes, new routes have been explored to make engineered carbon a profitable business. In this field, the most promising approach is probably the integration of carbon production with waste management [9–11]. The biomass waste stream is most abundant worldwide, and it is generally disposed through incineration. This represents both an environmental threat and an economic loss due to the transformation of a rich feedstock into heat and ashes. A more profitable approach is the thermal conversion of biomasses for the production of fuels [12,13], chemicals [14], and materials [15]. The conversion of biomass into liquid fuels is quite challenging due to the very high oxygen content of the original feedstock compared with traditional oil-derived fuel (i.e., gasoline and diesel). Nonetheless, the production of carbonaceous material from the thermochemical conversion of both lignocellulosic and non-lignocellulosic biomasses is very promising

for several reasons. This bioderived carbon is generally known as biochar and could be used for many applications [16], mainly due to its properties and well-balanced cost of around 0.8–2.4 €/kg [17–19]. Currently, the most common biochar application is as for soil health improvement [20–22] and for use as solid fuels with a heating content of around 40 kJ/mol [23]. These two applications are limited and do not exploit the many biochar applications that can be derived from its easy tuneability with simple process adjustment [24].

In this review paper, we report a comprehensive overview of the non-soil applications of biochar to prove its feasibility as a replacement for traditional carbon materials and as a solid competitor with high tech materials.

We summarize the recent literature in four main sections dedicated to (i) environmental remediation, (ii) energy storage, (iii) composite production, and (iv) other applications.

We hope that this review is an useful tool to navigate the great sea of biochar potential.

2. Biochar Production Strategies

Biochar is produced through four main thermochemical routes: (i) torrefaction, (ii) pyrolysis, (iii) hydrothermal carbonization and (iv) gasification.

Torrefaction is a low temperature thermal treatment that is used to densify biomasses for energy purposes [25]. The operative temperature ranges from 200 to 350 °C with long residence and processing times and high solid product yields [26]. The carbon content of solid residue is around 50–60 wt.% [27] but can reach 72–80 wt.% by using microwave heating combined with the addition of microwave susceptors [28–31]. This approach leads to the reduction of the process timescale to minutes.

Pyrolysis is a high temperature thermal treatment that breaks polymeric macromolecules, thus giving compounds that have a lower molecular weight in an oxygen free atmosphere [12,32]. Pyrolysis is run with different heating technologies [33] and apparatus designs [34–37] at a temperature range from 450 to 700 °C [38] with huge variations in product fraction yields.

Hydrothermal carbonization is a thermal depolymerization process that is used to convert wet biomass into crude-like oil, gas, and hydrochar under moderate temperature and high pressure [39] by using an aqueous solvent [40], a non-aqueous solvent [41,42] or sub-critical/critical media [43]. This process can be performed with [44] or without a catalyst [42], and it is useful for the improvement of properties of products [45].

Gasification is the conversion of biomass into a gaseous fuel by heating in a gasification medium such as air [46], oxygen, or steam [47], generally at temperatures higher than 800 °C with or without a catalyst [48]. Products from gasification are a mixture of carbon monoxide, carbon dioxide, methane, hydrogen and water vapor. Biochar that is produced from gasification processes shows a higher carbon and ash content compared to biochar from torrefaction and pyrolysis processes [49]. This was due to higher process temperatures that promote an advance cracking process with the simultaneous reduction of volatile organic matters and an increment of fixed carbon.

As shown in Figure 1, biochar carbon amount strongly correlates with the temperature that is adopted during the thermochemical conversion of all lignocellulosic biomasses.

Hydrogen/carbon and oxygen/carbon ratio low values are characteristic of less defective carbonaceous structures and could be more appealing for electronic and electric applications, while the other samples could be more useful as additive and for adsorptive processes [51,52].

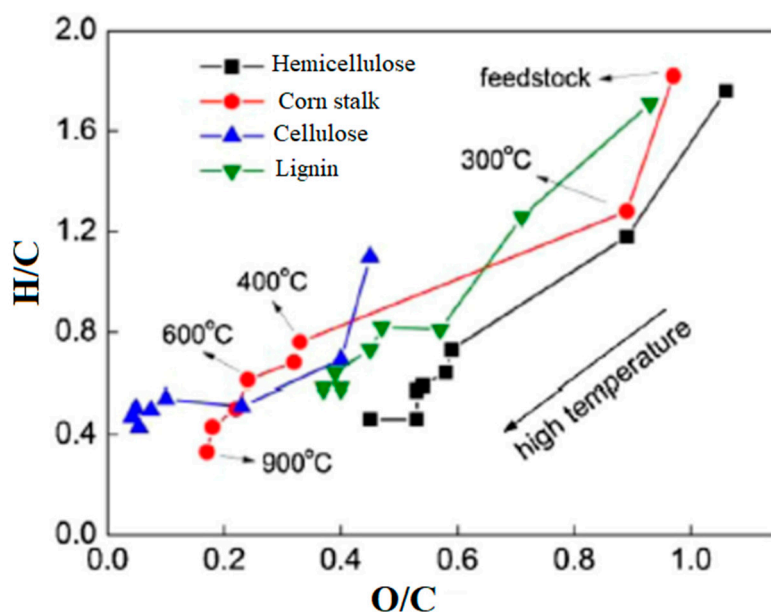


Figure 1. Van Krevelen diagram of corn stalk and corn stalk components during the thermochemical conversion process as reported by Gaojin et al. [50].

3. Non-Soil Biochar Applications

3.1. Environmental Remediation Applications

Environmental pollution is a global menace, and its magnitude is increasing day by day due to urbanization, heavy industrialization, and the changing lifestyles of people. In view of this, providing clean air, water and environments for people is a challenging task. In particular, the overall demand of water for human activities and the amount of wastewater that is produced are continuously increasing worldwide year by year [53]. Wastewater management has become one of the priorities for every urban conglomerate [54], involving several biological and chemical treatments [55] for reuse in civilian and industrial applications.

Water pollution is a global problem that is threatening the entire biosphere and affecting millions of lives [56]. Water pollution is recognized as one of the foremost global threats for human and environmental health [57]. A lot of different technologies for water purification are available based on filtration [58], adsorption [59], or degradation [60] technologies. Specialistic literature is rich in research that claims to have a water purification efficiency of up to 99%, but this is true only under idealized conditions of pH, contaminant concentrations, and other operating parameters [61]. Despite these astonishing claims, under real operative conditions, efficiency may substantially decrease. Furthermore, a lot of these techniques, such as ion exchange resins [62], are designed to target one class of contaminant at a time, which makes them useless in the case of environmentally polluted waters, where several contaminants simultaneously occur on a regular base. Taking into account these considerations, adsorption and degradative procedures are more appealing for real applications.

Biochar represents a game-changer material that is able to remove both inorganic and organic pollutants through adsorptive and degradative processes. Furthermore, biochar could be successfully used for air purification by removing molecules such as carbon dioxide or hydrogen disulfide.

3.1.1. Inorganic Pollutants Removal

Water pollution due to the presence of dissolved metal species has become a serious issue in a lot of underdeveloped [63–66] and developed countries [67,68]. The management of this issue is crucial for human health and safety.

Carbonaceous materials play a relevant role in the detoxification of watery sources, and biochar represents a very affordable solution. Huggins et al. [69] compared granular wood-derived biochar and granular-activated carbon for the treatment of a wastewater stream in both batch and column systems. The authors clearly showed that biochar-based filtering material reduces the total chemical oxygen demand (COD) and ion concentrations (PO_4^{3-} , NH_4^+ , As^{3+} , Cd^{2+} , Cr^{3+} , Pb^{2+} , Zn^{2+} , and Cu^{2+}) of wastewater treatment with more efficiency than activated carbon. Furthermore, biochar can be produced from so many feedstock sources that it guarantees a high versatility. Arán et al. [70] proved the relevance of feedstock by studying the copper adsorption of different feedstock-derived biochars. The authors clearly showed that the distribution of copper between the forms bound to biochar and dissolved into media depends on the starting material.

Chromium is a widely diffused element in the earth's crust that has found a lot of applications. Consequently, chromium pollution has arisen as a serious environmental issue due to its abundant emissions from refractory materials, stainless steel production, and steel alloy production [71]. Chromium(VI) is particularly toxic, and its removal is mandatory to avoid both environmental and human life threats. Currently, many adsorptive systems are available [72–74], but they are quite expensive. Biochar has been used for the removal of Cr(VI) in a very effective way. Banerjee et al. [75] developed a zirconium-caged steam-activated biochar for the removal of Cr(VI) by using a contaminated water flux/fixed bed approach. The authors claimed a high Cr(VI) removal efficiency of up to 94 wt.% under a moderate flux rate (4 mL/min).

Another promising approach taken by various researchers is based on redox methodology that converts Cr(VI) into Cr(III) after adsorption onto a carbonaceous structure [76]. In one study, this route was combined with a proposed one-pot solvothermal method that was applied to synthesize an iron-decorated magnetic biochar composite [77]. Biochar acted simultaneously as an adsorbent for Cr(VI) and an electron-donor for the reduction of Cr(VI) to Cr(III), while iron-containing nanoparticles were involved in the immobilization of Cr(III). Iron-decorated biochar showed a remarkable ability to remove chromium of up to 84 wt.% with an easy recoverability. Similarly, Shi et al. [78] tailored iron nanoparticles to be supported on a mixed system that was based on silica and biochar. The authors showed how the tailoring process improved the Cr(VI) adsorption ability by up to 28 mg/g for a final removal of up to 85 wt.%. The essential role of biochar in Cr(VI) reduction in Fe–biochar systems has been proven by systematic studies [79,80], as shown in Figure 2, while in another study, the conversion of Cr(VI) to Cr(III) was ascribed to the redox couple Fe(III)/Fe(II) present in the greigite mineral that was used to tailor a biochar surface [81].

Adsorption onto neat biochar particles was also used to purify water streams from Cd(II), Pb(II), Cu(II), Zn(II), Sm(III) [83–92].

Biochar surface modification plays a very relevant role on the adsorptive performances of biochar-based materials.

One of the most established procedures to magnify functionalities on a biochar surface is partial oxidation during or after pyrolytic treatment. A low-oxygen pyrolysis atmosphere (1%–4%) was used by Zhang et al. [93] with a significant Pb(II) removal increment from 17.2 to 71.7 wt.%. This was confirmed by the study reported by Gao et al. [94], who used an oxidative post-pyrolysis procedure-based treatment with HNO_3 , H_2O_2 or KMnO_4 . This functionalization led to a 97.4 wt.% sorption of Pb(II) from the watery solution. Liatsou et al. [95] showed, through a detailed set of investigations of herbaceous biochars treated with HNO_3 , that anhydrides and carboxylic acids act as main surface groups to bind metal ions.

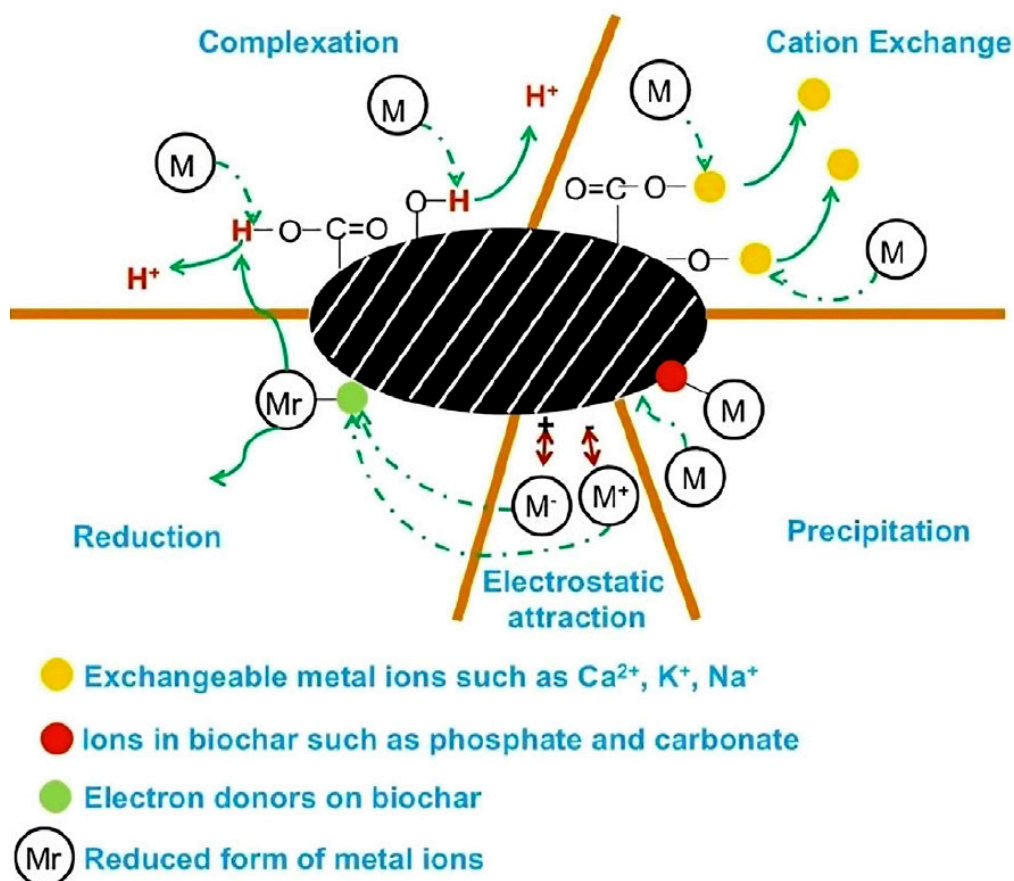


Figure 2. Mechanism of heavy metal adsorption onto neat biochar surface, as illustrated by Li et al. [82].

This assumption remains true for inorganic tailored biochar, as clearly showed by Feng et al. [96]. The authors described the effects of residual groups (i.e., hydroxyl, carbonyl, and carboxyl functionalities) on bromate removal when using a FeCl₃-decorated biochar. This study clearly showed that the main removal mechanism of bromate was due to the oxidation of hydroxyl groups while an Fe(III)/Fe(II) redox couple served as electron shuttle to facilitate the electron transfer.

Biochar iron decoration represents a very interesting approach to produce a performing and highly recoverable adsorbent material with complex interactions between iron and carbonaceous phases [97]. Zhang et al. [98] impregnated an apple pomace biochar with a solution of Fe(III)/Fe(II) and used it with successful results in the adsorption of a watery metal mixture. A step forward is represented by the study of Zhou et al. [99]; the authors prepared a urea-functionalized Fe(O)-decorated biochar that guaranteed a high removal and recovery efficiency during the adsorption of Cu(II). Guo et al. [100] combined iron with manganese oxides, achieving the recovery performance of the iron-tailored biochars, together with the ability to adsorb both Cr(II) and As(V). Further biochar tailoring processes have involved the introduction of phosphate residues that create a micropores structure together with a high surface area [101], as well as simple and complex organic [102,103] and inorganic [104,105] frameworks.

Anionic species that are dissolved in water represent another great family of watery pollutants; however, in this case, biochars still represent a valuable tool [106–109].

Phosphates are probably one of the principal causes of the eutrophication of surface waters [110–113]. Trazzi et al. [114] reported the use of a *Miscanthus* biochar produced at 700 °C for removing phosphates and segregating them into the soil, thus improving their agronomic performances and reducing algae proliferation.

Several biochar modifications have been used to tailor phosphorous uptake, ranging from electrochemical [115] to inorganic deposition [116,117] procedures. These studies led to the development

of real-scale plants based on biochar adsorbents that operate in flux and not merely on the batch scale [118].

Nitrate represents another anion species that is strongly correlated with eutrophication [119]. Divband et al. [120] developed a biochar from the pyrolysis of sugarcane bagasse, showing the best operative conditions after 1 h of using a solution with a pH of 4.64 and a starting nitrate concentration of up-to-a-dose-adsorbent of 2 g/L. Furthermore, species such as fluoride [121] and uranyl oxides [122,123] could be efficiently removed from watery phases by using biochar.

Biochar destiny after adsorption represents another strong point for its use for water purification. As reported by several authors [124,125], contaminated biochar could be a source of fertilizers, catalysis, metal nanoparticle synthesis through pyrolytic conversions, feed additives, and biologically active compounds.

The desalination process represents a further relevant application of water treatments that use biochar. This procedure has been performed through simple osmotic filtration [126] and through capacitive processes [127] with [128,129] or without [130] functionalization.

3.1.2. Organic Pollutants Removal

Watery pollution, due to the presence of organic molecules, has risen together with the anthropization. The anthropogenic effect is the main cause of the release of pollutants such as dyes, pharmaceuticals, and polymers residues [131,132]. During last few decades, the use of carbonaceous materials for the improvement of water purifications has been very intensively studied. Materials such as carbon dots [133], carbon nanotubes [134] and graphene [135] have been used for both organic pollutants detection and removal. Despite their performances, the high cost of high-tech carbon materials has slowed down their application in real-plant units.

Biochar represents a cheaper solution compared to other carbonaceous materials with very promising performances [136,137] due to the several interactions that occur on biochar particles, as summarized in Figure 3.

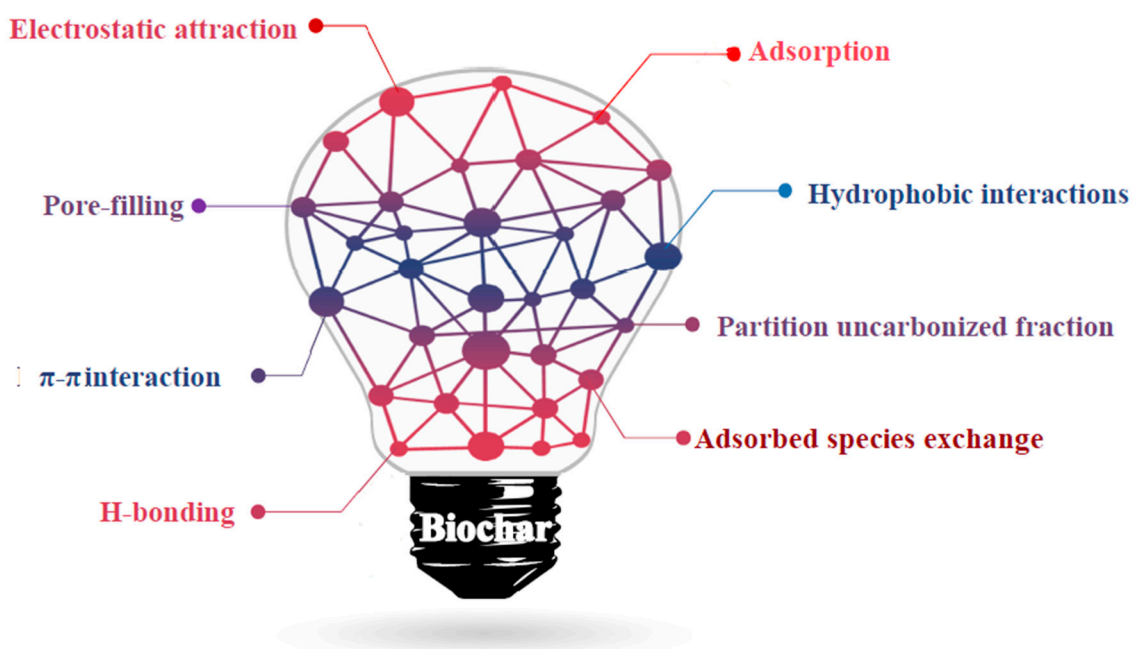


Figure 3. Schematic interactions occurring between organic molecules and biochar particles, as reported by Dai et al. [144].

The great variety of interactions that occur between biochar and organic molecules ranges from very weak (e.g., hydrophobic ones) to very strong (e.g., hydrogen bond and π - π orbital interactions).

The simultaneous occurrence of these interactions is the reason for the good performance of biochar as an adsorber for several typologies of compounds [138–143].

Firstly, biochar has been used to remove persistent small organic molecules such as aromatics. Jayawardhana et al. [145] used biochar that was derived from the pyrolysis of municipal solid waste to remove alkylated benzenes. They reached an efficiency of 850 and 550 $\mu\text{g/g}$ for toluene and m-xylene, respectively. Similarly, Kang et al. [146] used a biochar-derived material for the adsorption of phenanthrene. Nitroaromatics were also removed by using rice husk biochars, as described by Lingamdinne et al. [147]. In this research, the authors used a rice husk that had been pyrolyzed at 700 °C to remove 2,4,6-trinitrotoluene and 1,3,5-trinitro-1,3,5-triazacyclohexane. They showed that the adsorption process occurred through weak electrostatic interactions as well as through charge transfer between nitric functionalities and biochar surface functional groups. Mandal et al. [148] used various biomass wastes (tea, cucumber, and mixed hardwood) for the production of biochar at 400 and 700 °C. These carbonaceous materials were used to adsorb 2,4-dichlorophenoxy acetic acid, achieving an uptake of up to 59 mg/g. Zhu et al. [149] deeply investigated the interaction between biochar and 2,4-dichlorophenoxyacetic acid. They showed that surface amination and oxidation can improve biochar adsorption properties. Furthermore, polyhalogenated hydrocarbons were removed from waste stream by using biochar that was produced from the pyrolysis of digestate with an uptake of up to 11 mg/g [150].

Al Ameri et al. [151] used a peat-derived biochar as a bio-sorbent for the sorption and removal of crude oil spills from synthetic seawater, reaching a crude oil adsorption of 32.5 g per gram of biochar sorbent. Similarly, Feng et al. used porous carbon macro spheres with a diameter of 1–2 cm that were prepared through the carbonization of the fruit of *Liquidambar formosana*. The authors claimed an oil adsorption close to 99 wt.%.

Dyes represent the other great threat to water sanitation due to their persistency and toxicity [152]. The adsorption of dyes is affected by many parameters, such as solution pH, chemical nature and initial concentration of the dye molecules [153]. He et al. [154] reported the use of a micro-scale biochar particles/polysulfone mixed matrix hollow fiber membrane for the removal of methylene blue from water. The membrane's static and dynamic adsorption performance was investigated, and the adsorption mechanism was associated with electrostatic interaction, hydrogen bonding and hydrophobic interaction. In a study by Hou et al. [155], hydrochars from bamboo shoot shells were used for rhodamine B adsorption. Hydrochar produced at 800 °C with a heating rate of 25 °C adsorbed up to 86 mg/g of rhodamine B—a result that was lower than the results that were achieved by using non pyrolyzed sugar cane bagasse [156]. Zazycki et al. [157] used pecan nutshell biochar as low-cost adsorbent for removing Reactive Red 141 from aqueous solutions with an uptake of up to 130 mg/g, which was comparable with results achieved by Netpradit et al. [158], who used metal hydroxides. Jung et al. [159] produced a magnetic iron-decorated biochar from the pyrolysis of marine macroalgae for the adsorption of Orange 7 from aqueous media with comparable performances to those of metal frameworks [160]. The iron tailoring enabled a higher adsorption performance along with an easier separation and recovery process in the post-adsorption stage when using a simple magnet. A similar approach was applied by Heo et al. [161], who used a $\text{CuZnFe}_2\text{O}_4$ -tailored biochar composite for the simultaneous removal of bisphenol A and sulfamethoxazole.

Another rising issue in civilian water is the presence of traces of pharmaceuticals compounds due to their consumption [162,163] and inappropriate disposal [164]. Kim et al. [165] proposed an interesting ultrafiltration-activated biochar hybrid system for the removal of ibuprofen, 17 α -ethinyl estradiol, and carbamazepine, ultimately achieving an adsorption of up to 47 wt.%. Li et al. [166] used biochars that were prepared from cassava dregs at different pyrolytic temperatures (350, 450, and 700 °C) for the adsorption of ciprofloxacin, and this process is correlated to the action of residual groups with adsorption ability. Jang et al. [167] used a sodium hydroxide-activated biochar to remove tetracycline; a comparison with a commercial activated carbon (Calgon F400) showed a comparable activity with the biochar used. Similarly, Mandal et al. [168] removed atrazine and imidacloprid from water by

using an agricultural waste stream-derived biochar in a multi-staged batch adsorption systems. A different approach was reported by Xu and co-workers. They used Fe(0) nanoparticle-tailored biochar for the adsorption of florfenicol [169]. An additional sulfide modification of the iron nanoparticles led to the disruption of the antibiotic molecules.

Adsorption processes are neither the only nor the most used route to eliminate organic pollutants from watery streams. Degradative processes based on the oxidation routes play a major role in this field, mainly through catalytic-mediated peroxide oxidation, as shown in Figure 4.

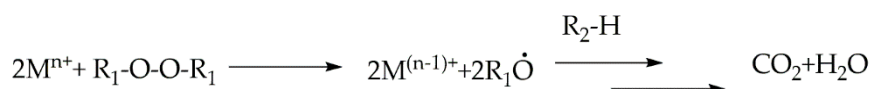


Figure 4. Schematic processes of the organic molecule degradation mediated by peroxides.

Fenton and Fenton-like processes are the more effective processes based on the activation of peroxides in mild conditions by using cheap metal precursors [170] and more stable oxidant agents such as persulfates [171]. Huang et al. [172] proved the significant role of biomass types on the formation of persistent free radicals during Fenton and Fenton-like process. This was particularly interesting because biochars have shown high catalytic potential due to their persistent free radicals that attract attention in the removal of refractory pollutants from water. The radical evolution in biochars that were derived from several biomasses (i.e., bamboo, corn stalk, and pig manure) were investigated by electron paramagnetic resonance. These experiments, together with linear sweep voltammetry measurements, showed that a hydroxyl radical was the dominant reactive radical in the biochar-H₂O₂ systems. Based on this study, He et al. [173] described persulfate activation with sawdust biochar in an aqueous solution with an enhanced electron donor-transfer effect. The authors pyrolyzed sawdust at two different temperatures (300 and 700 °C), showing that the degradation efficiency of Orange 7 increased along with the pyrolytic temperature. This was due to the graphite electron donor-transfer complex formed on the surface and in the pores of the biochar that played a decisive role in the reaction.

Interestingly, Ho et al. [174] produced a nitrogen-doped biochar from the pyrolysis of C-phycocyanin extracted spirulina residue for catalytic persulfate activation. The authors processed the feedstock at a high temperature (900 °C) and achieved nitrogen doping directly from the protein content. The resulting material promoted a non-radical activation process that guaranteed a mild and high-efficiency strategy for disinfection in waste and drinking water. More traditional catalysts that produced a porous biochar originated from *Myriophyllum aquaticum* tailored with Fe₃O₄ were described by Fu et al. [175]. This catalyst induced the activation of peroxymonosulfate during p-hydroxybenzoic acid degradation according to the traditional Fenton process route. Similarly, several authors have claimed the effectiveness of magnetic iron-based biochars in Fenton degradative processes [176,177]. Furthermore, Deng et al. described the use of pyrolyzed wood-waste for the fabrication of a porous carbon cathode that acts in the electro-Fenton degradative process of sulfathiazole in a pyrophosphate electrolyte alkaline environment. Bisphenol A could be also degraded by using both thermal [178] and ultrasound [179,180] induced Fenton processes.

Gan et al. [181] induced the degradation of refractive organic pollutants, such as dimethyl phthalate, by using a metal framework based on CoFe₂O₄ for the activation of peroxymonosulfate.

Fenton and Fenton-like routes are not the only available oxidative procedures. Moussavi et al. [182] prepared a biochar from a pistachio hull that demonstrated its catalytic potential for degrading Reactive Red 198 in catalytic ozonation processes, ultimately achieving a 58 wt.% removal efficiency.

Alternatively to oxidative degradation processes, reductive processes can also be performed, even if they are less appealing than the others due to their greater complexity. Some authors have described a reductive approach for the removal of nitro alkylated benzene based on the use of Fe(0)-tailored biochars [183,184], but the number of studies is still much lower than those on oxidative-based processes. A different and interesting approach is the hybrid system proposed by Lyu et al. [185] based on the use of biochar-supported nanoscale iron sulfide and *Corynebacterium variabile* HRJ4. The authors

applied this chemo-bio route for the dechlorination of trichloroethylene. A similar approach was used by Ayyappan et al. [186], who used a coconut shell biochar for dye degradation in a microbial fuel cell; they claimed a removal efficiency of up to 78 wt.%.

Photodegradative procedures have also been considered for watery streams purification [187]. Shirvanimoghadda et al. [188] produced and used carbon microtubes from the pyrolysis of cotton waste at different temperatures (from 900 to 1500 °C) for the UV photodegradation of bisphenol-A. A tailored magnetic biochar-containing Fe₃O₄-BiOBr was used by Li et al. [189] for carbamazepine photodegradation under visible LED light irradiation with a degradative performance of up to 96 wt.%. Kumar et al. [190] described another bismuth-based magnetic biochar material that was successfully used for the UV photodegradation of paraquat, with the nitrophenol reduction achieving a degradation of up to 99 wt.%. These performances were quite comparable with more expensive materials such as tailored graphene oxide [191]. Furthermore, the combination with cheap photoactive species such as zinc oxides has led to the realization of a performing photoactive material [192].

3.1.3. Gaseous Pollutants Removal

Gas mixture purification is one of the most relevant industrial issues [193]. Actually, the most used approaches are based on selective membranes [194,195] or in-solution absorption [196]. The use of a biochar-based adsorber could be an interesting application on a large scale for this bio waste-derived material. Das et al. [197] realized a biochar packed biofilter for gas-phase hydrogen sulfide removal; the authors claimed a very good stability for fifty days of operation. This system showed a maximum elimination capacity of 33 g/m³ h, along with a fast response to shock loads. A very similar approach was described by Braghiroli et al. [198] for the removal of SO₂ that was generated from anthropogenic sources. Shao et al. [199] used activated biochar, proving the beneficial effect of CO₂ activation in producing a material with a higher adsorption capability and a higher regenerability compared with pristine biochar.

Furthermore, the use of carbon dioxide as a biochar activation reagent could contribute to the reduction of CO₂ atmospheric emissions, which represent one of the greatest threat for climate change [200–202]. Nonetheless, the use of CO₂ for biochar activation is not the only route to mitigate emissions. The other and more appealing approach is represented by the use of biochar for the removal of CO₂ from gaseous mixtures [203]. Liu et al. [204] described the use of spent coffee grounds as efficient CO₂ adsorbers, reaching a gas uptake of up to 119 mg/g at 35 °C. Igalavithana et al. [205] recovered biochar from the gasification of food and wood waste, ultimately claiming a high CO₂ uptake and a very good recyclability. Huang et al. [206] used a biochar that was produced from the microwave co-torrefaction of sewage sludge and *Leucaena* wood, ultimately reaching a CO₂ uptake of up to 53 mg/g. Chiag et al. [207] explained different biochar CO₂ adsorption abilities with the surface microstructures and residual functionalities of carbonaceous materials. The effect of nitrogen residual functionalities was used by Zhang et al. [208] for the realization of a nitrogen-rich rice husk biochar that was able to adsorb CO₂ at a rate of 59 mg/g. Rice husk was also pyrolyzed under microwave irradiation [209] and activated with post-pyrolysis treatments [210], ultimately showing very promising CO₂ uptake values. Pyrolysis post-treatments were widely used to increase the CO₂ adsorption ability of a biochar by introducing basic sites via ammonia functionalization processes [211,212].

3.2. Energy Storage Applications

Energy storage technology represents a great challenge of 21st century [213] due to its different applications. Nowadays, numerous technologies [214] have been developed, such as solar and fuel cells [215,216], high performance batteries [217] and supercapacitors [218], as summarized in Figure 5.

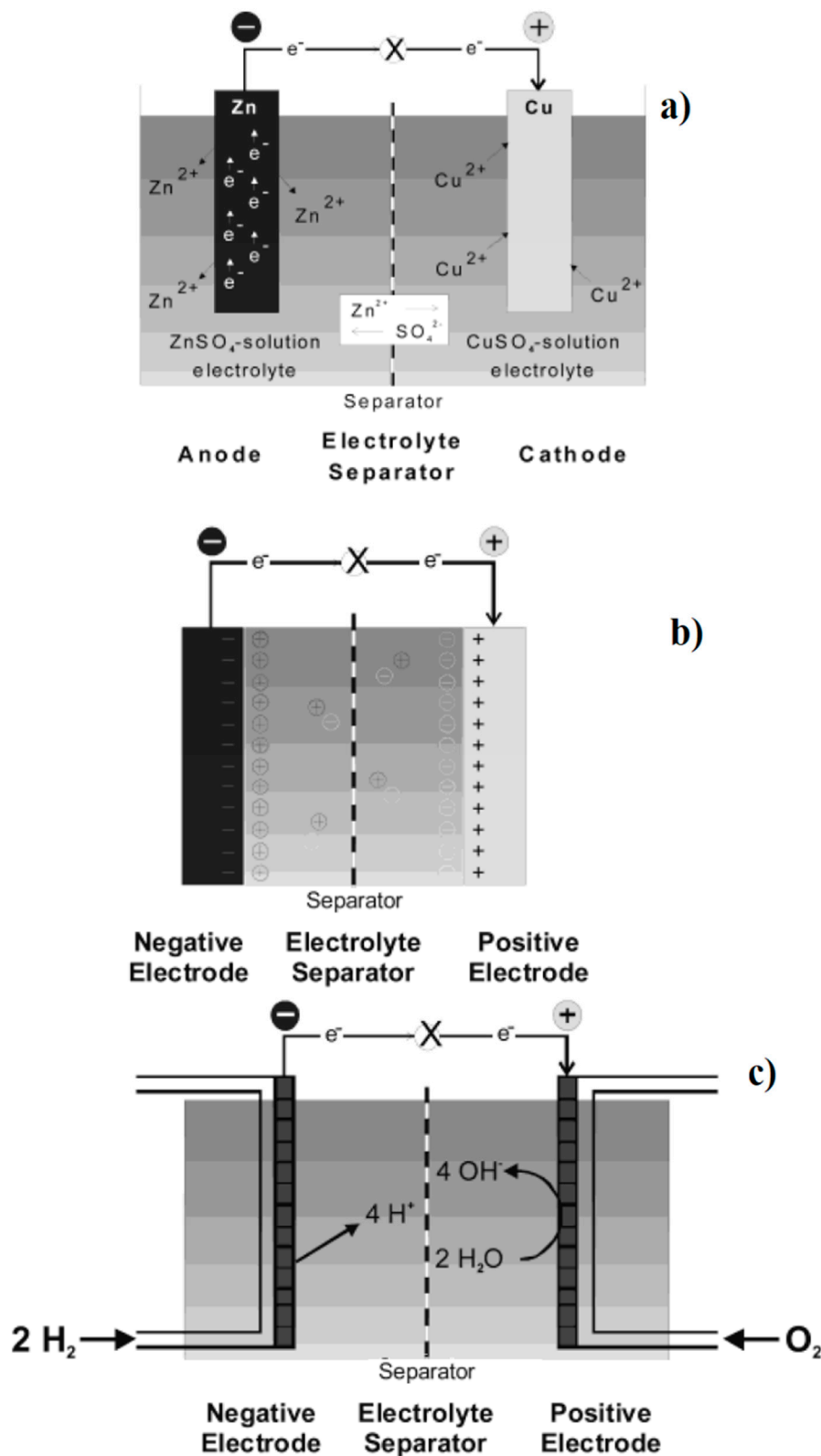


Figure 5. Schematic representation of (a) battery (Daniell cell), (b) a supercapacitor, and (c) a hydrogen fuel cell as reported by Winter et al. [219].

A battery is a system formed by at least two electrochemical cells with contacts to supply electrical energy according to electrochemical potential. Specialist literature has been focused on two main solid state battery systems based on lithium [220] and sodium [221] ions. A supercapacitor is an

energy storage modulus that stores energy in an electrical double layer that is formed at the interface between an electrolytic solution and an electronic conductor. A fuel cell is an electrochemical system that produces electric energy through the supply of a fuel (i.e., hydrogen [222], carbon [223], and methanol [224]) and an oxidant agent (i.e., oxygen and hydrogen peroxide).

3.2.1. Biochar Used for Supercapacitor Production

The essential requirement for producing a performing supercapacitor material is an elevated surface area where the double ionic layer can be created. For this purpose, physically- and chemically-activated biochar is a very attractive material for the realization of supercapacitor electrodes [225]. Chemical activation introduces functional groups on the surface of an activated biochar, thus affecting the latter's electrochemical properties [226]. Nonetheless, Gabhi et al. [227] described the effect of monolithic biochars with graphite and graphite-like structures on capacitive performance. The authors showed the relationships between conductivity and activate biochar structures at 950 °C by using sugar maple, oak and hickory woods. They claimed an increase of biochar conductivity from 5×10^{-6} up to 343 S/m when carbon content changed from 86.8 to 93.7 wt.%. This phenomenon was attributed to the formation of graphite nanocrystals in the main structure of the biochar during the high temperature treatment.

Chemical activation is a well-established procedure to create an activated biochar with a good capacitive performance. Luo et al. [228] reported cellulose activation by using ammonia, and they were able reach area capacitance of 40 mF/m².

Jin et al. [226] described the chemical activation of an ash-rich biochar by using potassium hydroxide at 900 °C, with a further modification occurring when using HNO₃ at 150 °C. Activated biochar showed a very high specific area of up to 2000 m²/g with a specific capacitance of up to 260 F/g.

A low ash content feedstock was used by Qu et al. [229] for a direct conversion into activated biochar by using a steam and acidic-alkali treatment. Corn-cob-activated biochar had a surface area of up to 1210 m²/g, a capacitance of 314 F/g, and a remarkable stability after 10⁵ cycles in a symmetrical cell. Fast pyrolysis and alkaline chemical activation was used by Chen et al. [230] for the conversion of rotten food waste into an activated biochar with a capacitance of 488 F/g. Herbaceous feedstocks were diffusely studied for electrodes production and feedstock like hemp [231] and several flowers [232,233] have been used for supercapacitor realization.

Surface morphology plays a relevant role in biochar-based supercapacitors [234–236]. As a matter of fact, macroporous biochar is characterized by an inferior performance compared to micro and mesoporous biochar, while microporous biochar has been shown to work at higher current density—up to 1.3 A/g—compared to other forms [237].

Activated biochar properties could be also modulated by using a plasma treatment, as described by Gupta et al. [238]. The authors reported a low temperature oxygen plasma treatment that was able to magnify the capacitance of a yellow pine biochar from 14 to 174 F/g as consequence of a surface area significant increment.

Furthermore, non-lignocellulosic biomasses could be converted into usefully carbonaceous materials for capacitive uses. As an example, keratin-mixed algae [239] was pyrolyzed for the production of heteroatom-doped activated biochar with interesting surface area and capacitive values. Pontiroli et al. [240] reported the production of a hierarchically-porous activated biochar from the pyrolysis of poultry litter with specific surface area of up to 3000 m²/g and a capacitance of 229 F/g.

3.2.2. Biochar Used for Batteries Production

Several authors have explored the use of biochars as anodic materials for the realization of performing batteries. Many authors have focused on the realization of lithium ion batteries due the great demand of highly technological devices based on them. Dai et al. [241] produced biochar from the pyrolysis of sewage sludge in order to produce hierarchical porous hollow carbon nanospheres with a great surface area of up to 1500 m²/g. This biochar was employed as an anode for an Li-ion battery and showed an impressive discharge capacity of up to 1169 mAh/g. Low porosity biochars

have shown far lower performances, as reported by Luna-Lama et al. [242], who used spent coffee grounds pyrolyzed at 800 °C and reached a specific capacity of only 360 mAh/g. This trend was confirmed by Zhang et al. [243], who reported values of around 600 mAh/g when using a microporous biochar. Similarly, Benitez et al. [244] reported the use of microporous biochar as a cathodic material for a lithium–sulfur battery with a specific capacity of 915 mAh/g and a current density of 100 mA/g. Chen et al. [245] showed that nitrogen doping could enhance hierarchical porous biochar activity derived from the pyrolysis of derived pomegranate residues at 700 °C of up to 550 mAh/g. Furthermore, the nitrogen-doped material was particularly stable after 500 cycles thanks to the chemical confinement of sulfur and the soluble lithium polysulfides performed by nitrogen sites. Heteroatom-doped biochar was used by Chen et al. [246] as a cathode with a discharge capacity of up to 1049 mAh/g. Non-lignocellulosic biomasses were used, as reported by Magnacca et al. [247]—the authors used chitin pyrolyzed at a moderate temperature for the realization of a low cost lithium–sulfur battery with acceptable performances. The tailoring process could further enhance biochar performance. Pan et al. [248] decorated a silk-derived biochar with nanocubes of ZnCo_2O_4 to produce a flexible performing anode material. Similarly, Li et al. [249] tailored a pomelo pericarp biochar with Fe_3O_4 nanoparticles, reaching a capacity of up to 635 mAh/g. Salimi et al. [250] combined the Fe_3O_4 nanoparticle-tailoring process with the pyrolysis of algae to produce an electrode material with a higher initial specific discharge capacity of up to 740 mAh/g and a good cyclic stability [251].

Different ion-based batteries have also been developed, though in minor quantities; the only solid works about is from Saavedra Rios et al. [252], who used biochars from various biomasses as precursors for hard carbon anodes in sodium-ion battery applications.

3.2.3. Biochar Used for Fuel Cell Production

Several authors [253–255] have used biochar as a fuel for direct carbon fuel cells, proving the relationship between biochar properties (e.g., carbon percentage, ash content, surface area, and heating value) and its fuel performances. Xu et al. [256] definitively established the direct relation between the thermal degradation of biomasses and their performances in carbon fuels cell by comparing thermogravimetric analysis with empirical data. Qiu et al. [257] reported the development of a direct carbon solid oxide fuel cell that was able to convert the chemical energy of biochar into electricity with high efficiency. The authors used biochar that had been derived from several biomasses (wheat straw, corncob, and bagasse), reaching a peak power densities of 260 mW/cm² at 800 °C. A detailed study of direct carbon fuel cells was reported by Kacprzak et al. [258–260]. Firstly, the authors compared graphite rod and biochar from an apple tree that was pyrolyzed at 600 °C in a molten salt mixture of sodium and potassium hydroxide, and they found an optimum operative condition at 400 °C with a NaOH/KOH ratio of 1. In these operative conditions, biochar outputs were comparable with those achieved when using pure graphite. A further experiment proved the similar behavior of biochar and commercial coal with a generated power, in both cases, close to 35 mW/cm².

In the same field, Ali et al. [261] used titanate-based anodes in a direct carbon fuel cell by using biochar from pyrolyzed walnut and almond shells as fuel. The authors claimed a generated power of up to 78 mW/cm². Elleuch et al. [262]—in similar conditions without the titanate-based anodes—reached a power of up to 127 mW/cm².

Another appealing use of biochar is the realization of electrodes for microbial fuel cells, as reported by Huggins et al. [263]. The authors used wood-based biochars as microbial fuel cell electrodes to significantly reduce costs and carbon footprints, showing a generated power of 532 ± 18 mW/m², with power cost of power output cost 17 \$/W. This was 90% cheaper than graphene-based fuel cell electrodes, which have a cost of up to 402 \$/W. Further improvements were achieved by using a manganese oxide-doped biochar, thus improving the power output by up to 606 mW/m² [264]. Khudzari et al. [265] developed a granular biochar anode in rice plant microbial fuel cells that were focused on the production of bioelectricity; the authors showed the beneficial effect of biochar on reducing methane emissions without decreasing plant biomass yield.

Biochar was also used for the production of performing cathode electrodes. Li et al. [266] produced biochar from the pyrolysis of corncob (with the temperature ranging from the torrefaction range up to 750 °C) that was used as an oxygen reduction reaction catalyst in air cathode microbial fuel cells; here, the biochar produced at 650 °C showed higher power outputs of up to 459 mW/m². Similarly, Yuan et al. [267] used a sewage sludge biochar produced at 900 °C to reach power outputs of up to 500 ± 17 mW/m².

Apart from the electrodes, Chakraborty et al. [268] developed a novel, low-cost proton exchange membrane that used sulfonated biochar that was produced from rotten food that had been pyrolyzed at 600 °C for application in microbial fuel cells. This study proved the high performances of the membrane, with a proton conductivity of 0.07 S/cm, an ion transport number of 0.891, and an oxygen diffusion coefficient of 6.5×10^{-9} m²/s. Comparing proton conductivity and power harvested per unit, the biochar-based membrane outperformed those based on materials such as Nafion.

3.3. Biochar-Based Composites Production and Properties

Nowadays, composite materials represent one of the largest global markets, with an expected future development of up to 131 billion dollars in 2024, as shown in Figure 6.

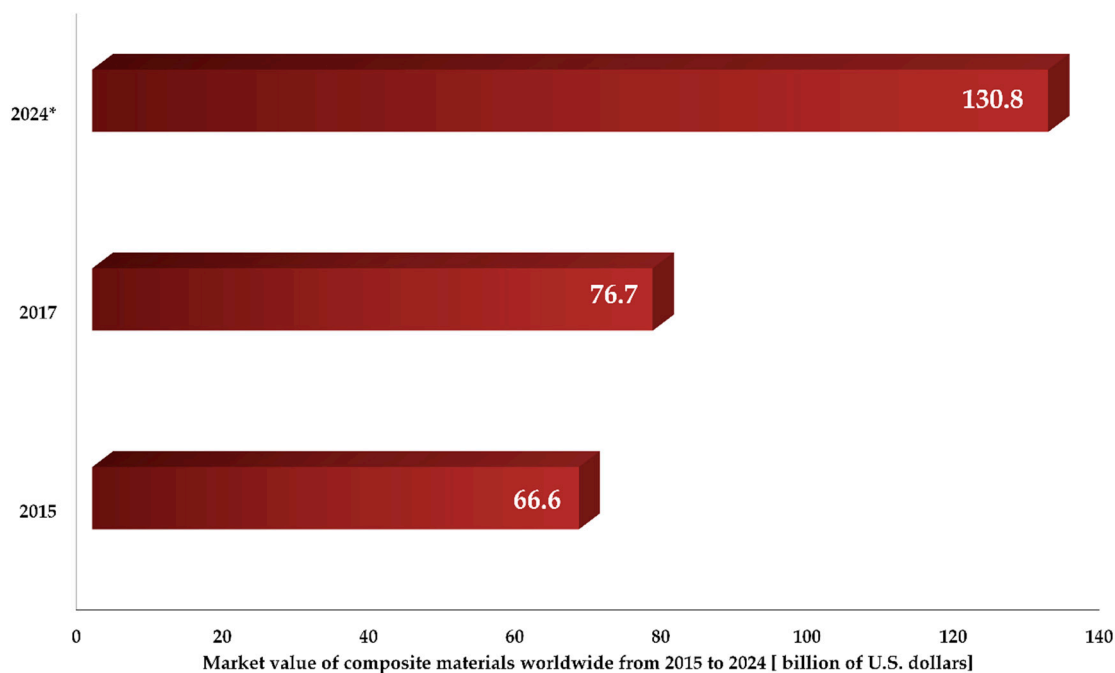


Figure 6. Composite material global market revenue, with a prediction for 2024 as reported by Grand Vie Research Center [269].

Carbon-based composites represent one of the most relevant parts of global markets, with an annual production of about 150 kton/y in 2018 [270]. As shown in Figure 7, around 70% of total carbon-based composites are represented by polymeric host materials, with 49.1% being thermoset and 29.5% being thermoplastic polymers. Among them, carbon fiber-reinforced epoxy resins represent a greater amount due to their many applications in key high-tech sectors such as aeronautics and aerospace industries [271]. Carbon-containing inorganic composites are mainly represented by ceramics [272] and cements [273], but their total production is far lower than polymers. In this scenario, biochar plays a minor role, even if its use is going to be consolidated due to production flexibility and its property tuneability [274].

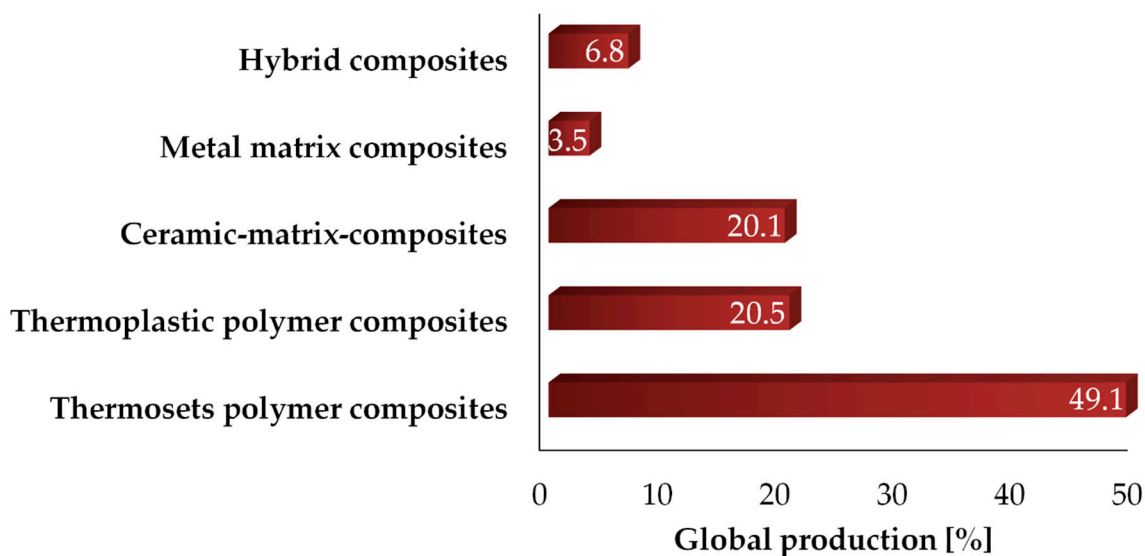


Figure 7. World carbon-based composite production in 2018, according to Sauer et al. [270].

3.3.1. Biochar–Inorganic-Based Composites

Cement production is one of the largest productions in the world, with more than 3 Gton/y produced in 2018 [275]. Along history, many additives have been developed to enhance both the mechanical properties and durability of cement-based material [276], ranging from polymers [277] to carbonaceous materials such as carbon nanotubes [278], graphene [279] and carbon fibers [280]. Biochar has also been extensively studied, even if it has not yet reached the market.

Cosentino et al. [281] evaluated the performance of a standardized biochar set that was produced by UK Biochar Research Center [282], considering flexural strength and fracture energy. The authors reported inferior performances compared to those achieved by previous studies [283]. Nonetheless, they reported a comprehensive study about the influence of a solid set of biochar properties (e.g., carbon content, pyrolysis temperature, and particle size) on the mechanical properties of biochar-containing cement composites. A further insight into biochar-based cement composites was reported by Gupta et al. [284]. The authors reported an exhaustive study on the influence of biochar particle size and surface morphology on the rheology, strength and permeability of cement mortar under both moist and dry curing conditions. The authors showed the primary effect of biochar macroporosity of big sized particles (diameters ranging from 2 to 100 μm) on the rheological properties of cement mortar. Biochar particle size did not affect the hydration process, which was fast in all experiments run. Small sized particles (diameters below 2 μm) improved early strength and water tightness compared to big size macroporous biochar particles. Mo et al. [285] combined biochar and MgO to mitigate the autogenous shrinkage of cement materials, and similar results were achieved by Muthukrishnan et al. [286] by simply using low-ash pyrolyzed rice husks. Gupta et al. [287] explored the addition of pre-soaked biochar particles that were produced at 500 $^{\circ}\text{C}$, and they showed a reduction of sorptivity and a depth of water penetration of up to 60%. Another interesting matrix that is able to host biochar is concrete. Concrete is more complex compared to neat cement, and it also contains inert material such as the sand of fine milled stones. The content of cement is highly variable and could partially or totally be replaced by biochar, as reported by Dixit et al. [288]. The authors described the use of biochar as a material for cement replacement in ultra-high performance concrete. The authors firstly described the biochar–concrete interphase interactions by using scanning electron microscopy to enlighten the deposition of cement hydrates on the surface and inside the surface pores of biochar, with dense interfacial transition zone, further suggesting the efficacy of biochar for improving hydration.

Gupta et al. [289] also proved that the addition of biochar that had been pyrolyzed at 550 $^{\circ}\text{C}$ improved concrete elevated temperature properties far better than fume silica, with a strength increment

of up to 20%. Biochar concrete composites showed interesting properties for the sound adsorption across the range of 200–2000 Hz, as reported by several research papers [290,291]. One of the most promising discoveries was comprised of the outputs presented by Kua et al. [292]. The authors described the use of biochar-immobilized bacteria mixed with poly(vinylalcohol) fibers for the production of a self-healing fiber-reinforced concrete. The authors claimed the ability of self-repairing cracks greater than 600 μm .

Cement and concrete are not the only inorganic matrixes that have been used to host biochar. Mu et al. [293] deeply described the use of carbon-containing clay composites as building materials. In this field, biochar has found many applications in construction science. Lee et al. [294] produced a hybrid material based on biochar and natural clay used as building envelope insulation with an increment to water vapor resistance due to the presence of up to 23 wt.% of biochar. The mechanical properties of biochar-based clay composites were described by Yang et al. [295]. The authors tested biochar that had been produced from several biomasses (e.g., rice husk, coconut shell, and bamboo) and showed an improvement in thermal performance and strength from a 10 wt.% mixture of bamboo-derived biochar and red clays.

Dahal et al. [296] used biochar as a filler in glass–fiber composites and showed lower damping ratio, an elevated storage moduli of up to 4 GPa, and a higher stiffness for the 10 wt.% biochar composite, as compared to the neat glass fibers.

3.3.2. Biochar-Containing Reinforced Plastics

Carbonaceous-reinforced thermoset plastics are widely diffuse materials that incorporate a plethora of different matrixes [297–299]. An epoxy matrix is the most studied and the most used matrix worldwide. Consequently, the replacement for traditional carbon fillers with biochar has stimulated great interest. Khan et al. [300] studied the mechanical and di-electrical properties of high-temperature annealed maple biochar-based epoxy composites by using a filler concentration ranging from 0.5 to 20 wt.%. The authors claimed a magnification of all mechanical properties when using an annealed biochar load of up to 4 wt.% and similar dielectric properties of low-loaded carbon nanotubes resin when using 20 wt.% of biochar. Bartoli et al. [301] established the relationship between the surface morphology of biochar particles and related composite mechanical properties by using a biochar loading of 2 wt.%. The authors achieved a 40% increment of maximum elongation when using a rhizomatous grass biochar and doubled the Young's modulus when using a wheat straw-derived biochar. The authors advanced the hypothesis that a smooth surface can induce an improved mobility inside the epoxy matrix, while a highly porous surfaces could not. This was reflected in the different behaviors that were observed when using biochar that was produced in the same pyrolytic conditions as different feedstocks.

Pyrolytic temperature plays a crucial role in the interactions between epoxy resins and biochar particles. Giorelli et al. [302] used a maple tree-derived biochar that was produced at 600 and 1000 °C, and they observed a maximum elongation improvement of up to five times compared with neat resin.

High temperature-treated biochar could be a solid choice for the production of conductive epoxy composites. Giorelli et al. [303] reported that more graphitized biochar showed a strong DC electrical conductivity. This affected the ability of these materials to shield the microwave radiation with a comparable performance to multiwalled carbon nanotubes [304], even as thin films [305].

Furthermore, biochar from pyrolyzed, wasted cotton fibers could be recovered in a carbon fiber shape that showed the property enhancement of an epoxy resin host matrix [306,307].

Regarding thermoplastic-reinforced plastics, polyolefins-based biochars are the most produced. Among them, biochar-containing polyethylene was studied by Arrigo et al. [308] by using a coffee-derived biochar. The authors reported that the rheological and thermal behavior of biochar composites showed a slowing down of the dynamics of the polymer host matrix due to the confinement of the polymer chains on the filler porous surface. Additionally, the well-embedded biochar particles improved the thermo-oxidative stability of the produced polyethylene composites. Zhang et al. [309]

studied the influence of temperature on poplar biochar-based high density polyethylene composites. Interestingly, the microcrystalline structure of the polymer matrix was not affected by the presence of biochar. On the other hand, the mechanical properties showed an appreciable difference between neat and biochar-loaded polymers, with the latter showing an improved flexural strength and a decreased impact strength. Li et al. [310] studied the behavior of highly biochar-loaded, ultra-high molecular weight polyethylene. The authors realized a performing electromagnetic interference shielding material by using 80 wt.% of bamboo biochar that was pyrolyzed at 1100 °C and reached a conductivity of 107.6 S/m. Furthermore, Bajwa et al. [311] reported the utilization of biochar for the production of a high density polyethylene/poly(lactic acid)/wood flour composites with super thermal stability properties.

Poly(propylene) is the other widely studied polyolefin for the realization of biochar-based composites. Das et al. [312] proved the economic feasibility of the use of biochar over traditional carbon fillers. The authors showed the cost reduction of biochar-based composites with the same properties of non-biochar-based ones due to the reduction of compatibilizer amounts of up to 3 wt.%, with 18 wt. % of saving. The low cost of biochar was the key of the study of Behazin et al. [313], where the authors used a pyrolyzed perennial for the realization of a poly(propylene)/poly(octene-ethylene) composite with filler loadings of 10 and 20 wt.%; they showed, through rheological analysis, stronger interactions between the polymer matrix and biochar. A detailed study of poly(propylene) and biochar interaction was reported by Bhattacharyya and co-workers in several papers [314–316]. During this research, the authors proved the general improvement of the mechanical and thermal properties of biochar-based poly(propylene) composites together with a significant effect in flame retardancy. Furthermore, Das et al. [317] produced biochar-based wood polymer composites while manufacturing a biocomposite with appreciable properties. Similarly, Poulouse et al. [318] combined date palm biochar with a poly(propylene) matrix and revealed that the biochar had negligible effect on the storage modulus up to a 15 wt.% loading. Other widely used polyolefin matrix used for the realization of piezo sensors are poly(vinyl alcohol) [319,320] and poly(acrylonitrile) [321].

Furthermore, polyesters were impregnated with biochar in a study by Ogunsona et al. [322]. The authors filled nylon 6 with biochar produced from the pyrolysis of *Miscanthus* at 500 and 900 °C, and they showed the beneficial effect of the high temperature-produced biochar and the detrimental effect of the other. Sheng et al. [323] modified bamboo biochars with silyl groups for the production of poly(lactic acid) composites, showing an enhancement of maximum elongation of up to 93% compared to a neat polymer.

Recently, biochar has been used for the production of biopolymer (i.e., starch [324] and gluten [325]) composites, thus fulfilling the vision of total bio and sustainable production.

3.4. Other Uses of Biochar

Biochar has found plenty of applications in all the field that are traditionally occupied by carbonaceous materials such as solid fuel [326,327]. The catalysis has seen the risen of biochar in the last few years [328], with application in many processes. Lee et al. [329] developed porous catalysts from pine and maize biochar that were produced at torrefaction temperatures ranging from 300 to 380 °C for biodiesel synthesis through a pseudo-catalytic transesterification. Li et al. [330] produced biochar from hydrolyze-mixed textile waste in the temperature range of 400–700 °C, and they used it as catalyst for succinic acid production in a fibrous bed bioreactor with a yield of 8 wt.%. The amount of surface acidic groups represent a key properties for biochar catalytic activity [331]. Kastner et al. [332] used a solid acid biochar as heterogenous catalyst for the esterification of fatty acids. Biochar produced at 500 °C was tailored with sulfonic groups to reach conversion values close to 99%. Zhong et al. [333] further tailored sulfonic-decorated biochar with alkyl groups, and they produced a highly active catalyst for biofuel production and for transesterification reactions [334].

Vidal et al. [335] developed an amino-siloxy-oxidized biochar that was able to promote the conversion of epoxy compounds and CO₂ into glycerol carbonate.

Areprasert et al. [336] introduced iron particles onto a biochar surface to perform catalytic reforming processes of waste electronic and electric equipment, reaching a liquid yield of up to 68 wt.%.

Furthermore, biochar could be efficiently used in redox-mediated reactions [337]. Cao et al. [338] proposed a very promising route to convert iron-enriched plant residue by using an electro-active biochar-based catalyst. The authors pyrolyzed a metal hyperaccumulator water plant and produced a biochar that contained 28 mg/g of iron. They tested the biochar that was produced in the electrocatalytic reduction of oxygenated water by using cyclic voltammetry, and they found a reduction current of up to 1.82 mA/cm².

Biochar could also be used for the production of electrochemical measurement devices [339,340]. Ziegler et al. [341] use mixed softwoods that were pyrolyzed at 700 °C with a drop-casting technique for the preparation of a room temperature-relative humidity sensor. The authors clearly showed the onset of the response, with a relative humidity of 5% varying the impedance of two orders of magnitude when humidity reached 100%. Similarly, Jagdale et al. [342] used spent coffee grounds to realize a relative humidity sensor with a starting response at 20% humidity. Further studies showed the use of biochar-based materials for the detection of ions (i.e., lead [343], copper [344], and zinc [345]) at concentrations of nmol/L and for organic materials in mmol/L concentrations [346,347]. Several authors have described the use of biochar-derived materials for biosensing. Kalinke et al. [348] pyrolyzed nitric acid-treated castor oil cake at 400 °C and tailored it with Ni(OH)₂/NiOOH for the realization of non-enzymatic glucose electrode. Alternatively, Martins et al. [349] developed an immunoassay for hantavirus detection that was based on a biochar platform with a range of work from 5 ng/mL to 1.0 µg/mL.

Biochar has also been used in biological procedures. Huang et al. [350] pyrolyzed rosin waste and tailored it with silver nanoparticles for anti-bacterial use. The use of biochar as additive in bioprocesses was reported by Bock et al. [351]. The authors used biochars to stabilize digestors because they control ammonia formation. Duan et al. [352] use biochar to improve short chain fatty acid algae anaerobic fermentation, and they doubled the amount of biomass production after four days.

4. Conclusions

In this review, we have presented an updated overview of non-soil applications of biochar with a focus on more useful and unusual ones. We reported many studies on the adsorptive capacity of ions and organic molecules, together with their biochar electrochemical properties. These properties are particularly relevant in the future perspective of clean energy production and storage. We also described, in detail, the possibility of using biochars as sound replacements for traditional fillers in both inorganic and organic composites materials. This evidence has shown the feasibility of the biochars used in a lot of sectors as solid alternatives to traditional and next-generation materials. The polyhedral nature of biochar represents a very strong advantage for spread the biochar use across material science field.

We hope that this summary of recent literature can lead to the foundation of new research which will exploit the great potential of biochar and biochar based materials.

Author Contributions: Conceptualization, M.B. and A.T.; writing—original draft preparation, M.B.; writing—review and editing, M.G., P.J., M.R., A.T.; visualization, M.B.; supervision, A.T.; project administration, A.T. All authors have read and agreed to the published version of the manuscript.

Funding: This research received no external funding.

Conflicts of Interest: The authors declare no conflict of interest.

References

1. Burchell, T.D. *Carbon Materials for Advanced Technologies*; Elsevier: Amsterdam, The Netherlands, 1999.
2. Holmes, M. Global carbon fibre market remains on upward trend. *Reinf. Plast.* **2014**, *58*, 38–45. [CrossRef]
3. Association, I.C.B. What is Carbon Black? Available online: <http://www.carbon-black.org/> (accessed on 17 December 2019).
4. Endo, M. Carbon nanotube research: Past and future. *Jpn. J. Appl. Phys.* **2012**, *51*, 040001.
5. Singh, V.; Joung, D.; Zhai, L.; Das, S.; Khondaker, S.I.; Seal, S. Graphene based materials: Past, present and future. *Prog. Mater. Sci.* **2011**, *56*, 1178–1271. [CrossRef]
6. Segal, M. Selling graphene by the ton. *Nat. Nanotechnol.* **2009**, *4*, 612. [CrossRef]
7. Tubes, C. Welcome To Cheap Tubes. Available online: <https://www.cheaptubes.com/> (accessed on 9 October 2019).
8. Alibaba.com. Market Price for Carbon Black n550. Available online: https://www.alibaba.com/product-detail/Market-price-for-carbon-black-n550_62080154763.html?spm=a2700.7724857.discountZoneStyleB_top.2.708e4ca9xSBebz (accessed on 14 November 2019).
9. Bezama, A.; Agamuthu, P. *Addressing the Big Issues in Waste Management*; SAGE Publications Sage UK: London, UK, 2019.
10. Mui, E.L.; Ko, D.C.; McKay, G. Production of active carbons from waste tyres—A review. *Carbon* **2004**, *42*, 2789–2805. [CrossRef]
11. Couth, R.; Trois, C. Carbon emissions reduction strategies in Africa from improved waste management: A review. *Waste Manag.* **2010**, *30*, 2336–2346. [CrossRef]
12. Bridgwater, A.V. Review of fast pyrolysis of biomass and product upgrading. *Biomass Bioenergy* **2012**, *38*, 68–94. [CrossRef]
13. Damartzis, T.; Zabaniotou, A. Thermochemical conversion of biomass to second generation biofuels through integrated process design—A review. *Renew. Sustain. Energy Rev.* **2011**, *15*, 366–378. [CrossRef]
14. Amen-Chen, C.; Pakdel, H.; Roy, C. Production of monomeric phenols by thermochemical conversion of biomass: A review. *Bioresour. Technol.* **2001**, *79*, 277–299. [CrossRef]
15. Paz-Ferreiro, J.; Nieto, A.; Méndez, A.; Askeland, M.P.J.; Gascó, G. Biochar from Biosolids Pyrolysis: A Review. *Int. J. Environ. Res. Public Health* **2018**, *15*, 956. [CrossRef] [PubMed]
16. Qian, K.; Kumar, A.; Zhang, H.; Bellmer, D.; Huhnke, R. Recent advances in utilization of biochar. *Renew. Sustain. Energy Rev.* **2015**, *42*, 1055–1064. [CrossRef]
17. Energy, F. Biochar: Prospects of Commercialization. Available online: <https://farm-energy.extension.org/> (accessed on 14 November 2019).
18. Vochozka, M.; Maroušková, A.; Váchal, J.; Straková, J. Biochar pricing hampers biochar farming. *Clean Technol. Environ. Policy* **2016**, *18*, 1225–1231. [CrossRef]
19. Maroušek, J. Significant breakthrough in biochar cost reduction. *Clean Technol. Environ. Policy* **2014**, *16*, 1821–1825. [CrossRef]
20. Ali, S.; Rizwan, M.; Qayyum, M.F.; Ok, Y.S.; Ibrahim, M.; Riaz, M.; Arif, M.S.; Hafeez, F.; Al-Wabel, M.I.; Shahzad, A.N. Biochar soil amendment on alleviation of drought and salt stress in plants: A critical review. *Environ. Sci. Pollut. Res.* **2017**, *24*, 12700–12712. [CrossRef]
21. Maroušek, J.; Strunecký, O.; Stehel, V. Biochar farming: Defining economically perspective applications. *Clean Technol. Environ. Policy* **2019**, 1389–1395. [CrossRef]
22. Maroušek, J.; Kolář, L.; Vochozka, M.; Stehel, V.; Maroušková, A. Biochar reduces nitrate level in red beet. *Environ. Sci. Pollut. Res.* **2018**, *25*, 18200–18203. [CrossRef]
23. Abdullah, H.; Wu, H. Biochar as a fuel: 1. Properties and grindability of biochars produced from the pyrolysis of mallee wood under slow-heating conditions. *Energy Fuels* **2009**, *23*, 4174–4181. [CrossRef]
24. Al-Wabel, M.I.; Al-Omran, A.; El-Naggar, A.H.; Nadeem, M.; Usman, A.R.A. Pyrolysis temperature induced changes in characteristics and chemical composition of biochar produced from conocarpus wastes. *Bioresour. Technol.* **2013**, *131*, 374–379. [CrossRef]

25. Chen, W.-H.; Peng, J.; Bi, X.T. A state-of-the-art review of biomass torrefaction, densification and applications. *Renew. Sustain. Energy Rev.* **2015**, *44*, 847–866. [[CrossRef](#)]
26. Gronnow, M.J.; Budarin, V.L.; Mašek, O.; Crombie, K.N.; Brownsort, P.A.; Shuttleworth, P.S.; Hurst, P.R.; Clark, J.H. Torrefaction/biochar production by microwave and conventional slow pyrolysis—comparison of energy properties. *Gcb Bioenergy* **2013**, *5*, 144–152. [[CrossRef](#)]
27. Bach, Q.-V.; Chen, W.-H.; Chu, Y.-S.; Skreiberg, Ø. Predictions of biochar yield and elemental composition during torrefaction of forest residues. *Bioresour. Technol.* **2016**, *215*, 239–246. [[CrossRef](#)] [[PubMed](#)]
28. Bartoli, M.; Rosi, L.; Giovannelli, A.; Frediani, P.; Frediani, M. Characterization of bio-oil and bio-char produced by low-temperature microwave-assisted pyrolysis of olive pruning residue using various absorbers. *Waste Manag. Res.* **2019**. [[CrossRef](#)] [[PubMed](#)]
29. Bartoli, M.; Rosi, L.; Giovannelli, A.; Frediani, P.; Frediani, M. Bio-oil from residues of short rotation coppice of poplar using a microwave assisted pyrolysis. *J. Anal. Appl. Pyrolysis* **2016**, *119*, 224–232. [[CrossRef](#)]
30. Bartoli, M.; Rosi, L.; Giovannelli, A.; Frediani, P.; Frediani, M. Pyrolysis of α -cellulose in a microwave multimode batch reactor. *J. Anal. Appl. Pyrolysis* **2016**, *120*, 284–296. [[CrossRef](#)]
31. Bartoli, M.; Rosi, L.; Giovannelli, A.; Frediani, P.; Frediani, M. Production of bio-oils and bio-char from *Arundo donax* through microwave assisted pyrolysis in a multimode batch reactor. *J. Anal. Appl. Pyrolysis* **2016**, *122*, 479–489. [[CrossRef](#)]
32. Wampler, T.P. *Applied Pyrolysis Handbook*; CRC Press: Boca Raton, FL, USA, 2006.
33. Bridgwater, A.; Peacocke, G. Fast pyrolysis processes for biomass. *Renew. Sustain. Energy Rev.* **2000**, *4*, 1–73. [[CrossRef](#)]
34. Ragucci, R.; Giudicianni, P.; Cavaliere, A. Cellulose slow pyrolysis products in a pressurized steam flow reactor. *Fuel* **2013**, *107*, 122–130. [[CrossRef](#)]
35. Tsai, W.; Lee, M.; Chang, Y. Fast pyrolysis of rice straw, sugarcane bagasse and coconut shell in an induction-heating reactor. *J. Anal. Appl. Pyrolysis* **2006**, *76*, 230–237. [[CrossRef](#)]
36. Karaduman, A.; Şimşek, E.H.; Çiçek, B.; Bilgesü, A.Y. Flash pyrolysis of polystyrene wastes in a free-fall reactor under vacuum. *J. Anal. Appl. Pyrolysis* **2001**, *60*, 179–186. [[CrossRef](#)]
37. Li, D.; Briens, C.; Berruti, F. Improved lignin pyrolysis for phenolics production in a bubbling bed reactor—Effect of bed materials. *Bioresour. Technol.* **2015**, *189*, 7–14. [[CrossRef](#)]
38. Horne, P.A.; Williams, P.T. Influence of temperature on the products from the flash pyrolysis of biomass. *Fuel* **1996**, *75*, 1051–1059. [[CrossRef](#)]
39. Behrendt, F.; Neubauer, Y.; Oevermann, M.; Wilmes, B.; Zobel, N. Direct Liquefaction of Biomass. *Chem. Eng. Technol.* **2008**, *31*, 667–677. [[CrossRef](#)]
40. Akhtar, J.; Amin, N.A.S. A review on process conditions for optimum bio-oil yield in hydrothermal liquefaction of biomass. *Renew. Sustain. Energy Rev.* **2011**, *15*, 1615–1624. [[CrossRef](#)]
41. Liu, Z.; Zhang, F.-S. Effects of various solvents on the liquefaction of biomass to produce fuels and chemical feedstocks. *Energy Convers. Manag.* **2008**, *49*, 3498–3504. [[CrossRef](#)]
42. Zou, S.; Wu, Y.; Yang, M.; Li, C.; Tong, J. Thermochemical catalytic liquefaction of the marine microalgae *Dunaliella tertiolecta* and characterization of bio-oils. *Energy Fuels* **2009**, *23*, 3753–3758. [[CrossRef](#)]
43. Peterson, A.A.; Vogel, F.; Lachance, R.P.; Fröling, M.; Antal, M.J., Jr.; Tester, J.W. Thermochemical biofuel production in hydrothermal media: A review of sub- and supercritical water technologies. *Energy Environ. Sci.* **2008**, *1*, 32–65. [[CrossRef](#)]
44. Mok, W.S.L.; Antal, M.J., Jr. Uncatalyzed solvolysis of whole biomass hemicellulose by hot compressed liquid water. *Ind. Eng. Chem. Res.* **1992**, *31*, 1157–1161. [[CrossRef](#)]

45. Zhong, C.; Wei, X. A comparative experimental study on the liquefaction of wood. *Energy* **2004**, *29*, 1731–1741. [[CrossRef](#)]
46. Guizani, C.; Sanz, F.E.; Salvador, S. Influence of temperature and particle size on the single and mixed atmosphere gasification of biomass char with H₂O and CO₂. *Fuel Process. Technol.* **2015**, *134*, 175–188. [[CrossRef](#)]
47. Barisano, D.; Canneto, G.; Nanna, F.; Alvino, E.; Pinto, G.; Villone, A.; Carnevale, M.; Valerio, V.; Battafarano, A.; Braccio, G. Steam/oxygen biomass gasification at pilot scale in an internally circulating bubbling fluidized bed reactor. *Fuel Process. Technol.* **2016**, *141*, 74–81. [[CrossRef](#)]
48. Cheah, S.; Jablonski, W.S.; Olstad, J.L.; Carpenter, D.L.; Barthelemy, K.D.; Robichaud, D.J.; Andrews, J.C.; Black, S.K.; Oddo, M.D.; Westover, T.L. Effects of thermal pretreatment and catalyst on biomass gasification efficiency and syngas composition. *Green Chem.* **2016**, *18*, 6291–6304. [[CrossRef](#)]
49. Brewer, C.E.; Schmidt-Rohr, K.; Satrio, J.A.; Brown, R.C. Characterization of biochar from fast pyrolysis and gasification systems. *Environ. Prog. Sustain. Energy* **2009**, *28*, 386–396. [[CrossRef](#)]
50. Lv, G.; Wu, S.; Yang, G.; Chen, J.; Liu, Y.; Kong, F. Comparative study of pyrolysis behaviors of corn stalk and its three components. *J. Anal. Appl. Pyrolysis* **2013**, *104*, 185–193. [[CrossRef](#)]
51. Truong, H.B.; Ike, I.A.; Ok, Y.S.; Hur, J. Polyethyleneimine modification of activated fly ash and biochar for enhanced removal of natural organic matter from water via adsorption. *Chemosphere* **2020**, *243*, 125454–125483. [[CrossRef](#)]
52. Zhang, H.; Wang, T.; Sui, Z.; Zhang, Y.; Sun, B.; Pan, W.-P. Enhanced mercury removal by transplanting sulfur-containing functional groups to biochar through plasma. *Fuel* **2019**, *253*, 703–712. [[CrossRef](#)]
53. Seckler, D.W. *World Water Demand and Supply, 1990 to 2025: Scenarios and Issues*; Iwmi: Colombo, Sri Lanka, 1998; Volume 19.
54. Connor, R. *Wastewater: The Untapped Resource*; United Nations Educational, Scientific and Cultural Organization: Paris, France, 2017.
55. Ramalho, R. *Introduction to Wastewater Treatment Processes*; Elsevier: Amsterdam, The Netherlands, 2012.
56. Cassivi, A.; Guilherme, S.; Bain, R.; Tilley, E.; Waygood, E.O.D.; Dorea, C. Drinking water accessibility and quantity in low and middle-income countries: A systematic review. *Int. J. Hyg. Environ. Health* **2019**, *222*, 1011–1020. [[CrossRef](#)]
57. Goel, P. *Water Pollution: Causes, Effects and Control*; New Age International: Delhi, India, 2006.
58. Pendergast, M.M.; Hoek, E.M. A review of water treatment membrane nanotechnologies. *Energy Environ. Sci.* **2011**, *4*, 1946–1971. [[CrossRef](#)]
59. Rafatullah, M.; Sulaiman, O.; Hashim, R.; Ahmad, A. Adsorption of methylene blue on low-cost adsorbents: A review. *J. Hazard. Mater.* **2010**, *177*, 70–80. [[CrossRef](#)]
60. Neyens, E.; Baeyens, J. A review of classic Fenton's peroxidation as an advanced oxidation technique. *J. Hazard. Mater.* **2003**, *98*, 33–50. [[CrossRef](#)]
61. Hillie, T.; Hlophe, M. Nanotechnology and the challenge of clean water. *Nat. Nanotechnol.* **2007**, *2*, 663. [[CrossRef](#)]
62. Fu, F.; Wang, Q. Removal of heavy metal ions from wastewaters: A review. *J. Environ. Manag.* **2011**, *92*, 407–418. [[CrossRef](#)] [[PubMed](#)]
63. Gowd, S.S.; Govil, P.K. Distribution of heavy metals in surface water of Ranipet industrial area in Tamil Nadu, India. *Environ. Monit. Assess.* **2008**, *136*, 197–207. [[CrossRef](#)] [[PubMed](#)]
64. Zheng, J.; Chen, K.-H.; Yan, X.; Chen, S.-J.; Hu, G.-C.; Peng, X.-W.; Yuan, J.-G.; Mai, B.-X.; Yang, Z.-Y. Heavy metals in food, house dust, and water from an e-waste recycling area in South China and the potential risk to human health. *Ecotoxicol. Environ. Saf.* **2013**, *96*, 205–212. [[CrossRef](#)] [[PubMed](#)]
65. Szymanowska, A.; Samecka-Cymerman, A.; Kempers, A. Heavy metals in three lakes in West Poland. *Ecotoxicol. Environ. Saf.* **1999**, *43*, 21–29. [[CrossRef](#)]
66. Karadede, H.; Ünlü, E. Concentrations of some heavy metals in water, sediment and fish species from the Atatürk Dam Lake (Euphrates), Turkey. *Chemosphere* **2000**, *41*, 1371–1376. [[CrossRef](#)]

67. Nriagu, J.O.; Wong, H.K.; Lawson, G.; Daniel, P. Saturation of ecosystems with toxic metals in Sudbury basin, Ontario, Canada. *Sci. Total Environ.* **1998**, *223*, 99–117. [[CrossRef](#)]
68. Ikem, A.; Egiebor, N.; Nyavor, K. Trace elements in water, fish and sediment from Tuskegee Lake, Southeastern USA. *Water/air/soil Pollut.* **2003**, *149*, 51–75. [[CrossRef](#)]
69. Huggins, T.M.; Haeger, A.; Biffinger, J.C.; Ren, Z.J. Granular biochar compared with activated carbon for wastewater treatment and resource recovery. *Water Res.* **2016**, *94*, 225–232. [[CrossRef](#)]
70. Arán, D.; Antelo, J.; Fiol, S.; Macías, F. Influence of feedstock on the copper removal capacity of waste-derived biochars. *Bioresour. Technol.* **2016**, *212*, 199–206. [[CrossRef](#)]
71. Towill, L.E.; Shriner, C.; Drury, J.; Hammons, A.; Holleman, J. *Reviews of the Environmental Effects of Pollutants. III. Chromium*; Oak Ridge National Lab.: Oak Ridge, TN, USA, 1978.
72. Rengaraj, S.; Yeon, K.-H.; Moon, S.-H. Removal of chromium from water and wastewater by ion exchange resins. *J. Hazard. Mater.* **2001**, *87*, 273–287. [[CrossRef](#)]
73. Brum, M.C.; Capitaneo, J.L.; Oliveira, J.F. Removal of hexavalent chromium from water by adsorption onto surfactant modified montmorillonite. *Miner. Eng.* **2010**, *23*, 270–272. [[CrossRef](#)]
74. Gifford, M.; Hristovski, K.; Westerhoff, P. Ranking traditional and nano-enabled sorbents for simultaneous removal of arsenic and chromium from simulated groundwater. *Sci. Total Environ.* **2017**, *601*, 1008–1014. [[CrossRef](#)] [[PubMed](#)]
75. Banerjee, S.; Joshi, S.R.; Mandal, T.; Halder, G. Application of zirconium caged activated biochar alginate beads towards deionization of Cr(VI) laden water in a fixed bed column reactor. *J. Environ. Chem. Eng.* **2018**, *6*, 4018–4029. [[CrossRef](#)]
76. Zhou, L.; Deng, H.; Wan, J.; Shi, J.; Su, T. A solvothermal method to produce RGO-Fe₃O₄ hybrid composite for fast chromium removal from aqueous solution. *Appl. Surf. Sci.* **2013**, *283*, 1024–1031. [[CrossRef](#)]
77. Liang, S.; Shi, S.; Zhang, H.; Qiu, J.; Yu, W.; Li, M.; Gan, Q.; Yu, W.; Xiao, K.; Liu, B.; et al. One-pot solvothermal synthesis of magnetic biochar from waste biomass: Formation mechanism and efficient adsorption of Cr(VI) in an aqueous solution. *Sci. Total Environ.* **2019**, *695*, 133886. [[CrossRef](#)]
78. Shi, S.; Yang, J.; Liang, S.; Li, M.; Gan, Q.; Xiao, K.; Hu, J. Enhanced Cr(VI) removal from acidic solutions using biochar modified by Fe₃O₄@SiO₂-NH₂ particles. *Sci. Total Environ.* **2018**, *628*, 499–508. [[CrossRef](#)]
79. Wang, K.; Sun, Y.; Tang, J.; He, J.; Sun, H. Aqueous Cr(VI) removal by a novel ball milled Fe₀-biochar composite: Role of biochar electron transfer capacity under high pyrolysis temperature. *Chemosphere* **2019**. [[CrossRef](#)]
80. Xu, X.; Huang, H.; Zhang, Y.; Xu, Z.; Cao, X. Biochar as both electron donor and electron shuttle for the reduction transformation of Cr(VI) during its sorption. *Environ. Pollut.* **2019**, *244*, 423–430. [[CrossRef](#)]
81. Wang, X.; Xu, J.; Liu, J.; Liu, J.; Xia, F.; Wang, C.; Dahlgren, R.A.; Liu, W. Mechanism of Cr(VI) removal by magnetic greigite/biochar composites. *Sci. Total Environ.* **2019**. [[CrossRef](#)]
82. Li, H.; Dong, X.; da Silva, E.B.; de Oliveira, L.M.; Chen, Y.; Ma, L.Q. Mechanisms of metal sorption by biochars: Biochar characteristics and modifications. *Chemosphere* **2017**, *178*, 466–478. [[CrossRef](#)]
83. Álvarez-Rogel, J.; Tercero Gómez, M.d.C.; Conesa, H.M.; Párraga-Aguado, I.; González-Alcaraz, M.N. Biochar from sewage sludge and pruning trees reduced porewater Cd, Pb and Zn concentrations in acidic, but not basic, mine soils under hydric conditions. *J. Environ. Manag.* **2018**, *223*, 554–565. [[CrossRef](#)] [[PubMed](#)]
84. Cataldo, S.; Chiodo, V.; Crea, F.; Maisano, S.; Milea, D.; Pettignano, A. Biochar from byproduct to high value added material—A new adsorbent for toxic metal ions removal from aqueous solutions. *J. Mol. Liq.* **2018**, *271*, 481–489. [[CrossRef](#)]
85. Chen, Z.-L.; Zhang, J.-Q.; Huang, L.; Yuan, Z.-H.; Li, Z.-J.; Liu, M.-C. Removal of Cd and Pb with biochar made from dairy manure at low temperature. *J. Integr. Agric.* **2019**, *18*, 201–210. [[CrossRef](#)]
86. Deng, Y.; Huang, S.; Laird, D.A.; Wang, X.; Meng, Z. Adsorption behaviour and mechanisms of cadmium and nickel on rice straw biochars in single- and binary-metal systems. *Chemosphere* **2019**, *218*, 308–318. [[CrossRef](#)]
87. Hadjittofi, L.; Charalambous, S.; Pashalidis, I. Removal of trivalent samarium from aqueous solutions by activated biochar derived from cactus fibres. *J. Rare Earths* **2016**, *34*, 99–104. [[CrossRef](#)]

88. Kołodyńska, D.; Wnętrzak, R.; Leahy, J.J.; Hayes, M.H.B.; Kwapiński, W.; Hubicki, Z. Kinetic and adsorptive characterization of biochar in metal ions removal. *Chem. Eng. J.* **2012**, *197*, 295–305. [[CrossRef](#)]
89. Pal, D.; Maiti, S.K. Abatement of cadmium (Cd) contamination in sediment using tea waste biochar through meso-microcosm study. *J. Clean. Prod.* **2019**, *212*, 986–996. [[CrossRef](#)]
90. Li, M.; Liu, Q.; Guo, L.; Zhang, Y.; Lou, Z.; Wang, Y.; Qian, G. Cu(II) removal from aqueous solution by *Spartina alterniflora* derived biochar. *Bioresour. Technol.* **2013**, *141*, 83–88. [[CrossRef](#)]
91. Tong, X.; Xu, R. Removal of Cu(II) from acidic electroplating effluent by biochars generated from crop straws. *J. Environ. Sci.* **2013**, *25*, 652–658. [[CrossRef](#)]
92. Wang, H.; Zhang, M.; Lv, Q. Influence of Pyrolysis Temperature on Cadmium Removal Capacity and Mechanism by Maize Straw and Platanus Leaves Biochars. *Int. J. Environ. Res. Public Health* **2019**, *16*, 845. [[CrossRef](#)]
93. Zhang, C.; Shan, B.; Tang, W.; Zhu, Y. Comparison of cadmium and lead sorption by *Phyllostachys pubescens* biochar produced under a low-oxygen pyrolysis atmosphere. *Bioresour. Technol.* **2017**, *238*, 352–360. [[CrossRef](#)] [[PubMed](#)]
94. Gao, R.; Xiang, L.; Hu, H.; Fu, Q.; Zhu, J.; Liu, Y.; Huang, G. High-efficiency removal capacities and quantitative sorption mechanisms of Pb by oxidized rape straw biochars. *Sci. Total Environ.* **2019**. [[CrossRef](#)] [[PubMed](#)]
95. Liatsou, I.; Pashalidis, I.; Oezaslan, M.; Dosche, C. Surface characterization of oxidized biochar fibers derived from *Luffa Cylindrica* and lanthanide binding. *J. Environ. Chem. Eng.* **2017**, *5*, 4069–4074. [[CrossRef](#)]
96. Feng, Z.; Chen, N.; Feng, C.; Fan, C.; Wang, H.; Deng, Y.; Gao, Y. Roles of functional groups and irons on bromate removal by FeCl₃ modified porous carbon. *Appl. Surf. Sci.* **2019**, *488*, 681–687. [[CrossRef](#)]
97. Zhu, L.; Tong, L.; Zhao, N.; Li, J.; Lv, Y. Coupling interaction between porous biochar and nano zero valent iron/nano α -hydroxyl iron oxide improves the remediation efficiency of cadmium in aqueous solution. *Chemosphere* **2019**, *219*, 493–503. [[CrossRef](#)] [[PubMed](#)]
98. Zhang, S.; Ji, Y.; Dang, J.; Zhao, J.; Chen, S. Magnetic apple pomace biochar: Simple preparation, characterization, and application for enriching Ag(I) in effluents. *Sci. Total Environ.* **2019**, *668*, 115–123. [[CrossRef](#)]
99. Zhou, X.; Liu, Y.; Zhou, J.; Guo, J.; Ren, J.; Zhou, F. Efficient removal of lead from aqueous solution by urea-functionalized magnetic biochar: Preparation, characterization and mechanism study. *J. Taiwan Inst. Chem. Eng.* **2018**, *91*, 457–467. [[CrossRef](#)]
100. Guo, J.; Yan, C.; Luo, Z.; Fang, H.; Hu, S.; Cao, Y. Synthesis of a novel ternary HA/Fe-Mn oxides-loaded biochar composite and its application in cadmium(II) and arsenic(V) adsorption. *J. Environ. Sci.* **2019**, *85*, 168–176. [[CrossRef](#)]
101. Hu, R.; Xiao, J.; Wang, T.; Chen, G.; Chen, L.; Tian, X. Engineering of phosphate-functionalized biochars with highly developed surface area and porosity for efficient and selective extraction of uranium. *Chem. Eng. J.* **2020**, *379*, 122388. [[CrossRef](#)]
102. Li, M.; Wei, D.; Liu, T.; Liu, Y.; Yan, L.; Wei, Q.; Du, B.; Xu, W. EDTA functionalized magnetic biochar for Pb(II) removal: Adsorption performance, mechanism and SVM model prediction. *Sep. Purif. Technol.* **2019**, *227*, 115696. [[CrossRef](#)]
103. Lyu, H.; Xia, S.; Tang, J.; Zhang, Y.; Gao, B.; Shen, B. Thiol-modified biochar synthesized by a facile ball-milling method for enhanced sorption of inorganic Hg²⁺ and organic CH₃Hg⁺. *J. Hazard. Mater.* **2019**. [[CrossRef](#)] [[PubMed](#)]
104. Jellali, S.; Diamantopoulos, E.; Haddad, K.; Anane, M.; Durner, W.; Mlayah, A. Lead removal from aqueous solutions by raw sawdust and magnesium pretreated biochar: Experimental investigations and numerical modelling. *J. Environ. Manag.* **2016**, *180*, 439–449. [[CrossRef](#)] [[PubMed](#)]

105. Shih, Y.-J.; Dong, C.-D.; Huang, Y.-H.; Huang, C.P. Electro-sorption of ammonium ion onto nickel foam supported highly microporous activated carbon prepared from agricultural residues (dried *Luffa cylindrica*). *Sci. Total Environ.* **2019**, *673*, 296–305. [[CrossRef](#)] [[PubMed](#)]
106. Li, X.; Zhao, C.; Zhang, M. Chapter 8-Biochar for Anionic Contaminants Removal From Water. In *Biochar from Biomass and Waste*; Ok, Y.S., Tsang, D.C.W., Bolan, N., Novak, J.M., Eds.; Elsevier: Amsterdam, The Netherlands, 2019; pp. 143–160. [[CrossRef](#)]
107. Li, R.; Wang, J.J.; Gaston, L.A.; Zhou, B.; Li, M.; Xiao, R.; Wang, Q.; Zhang, Z.; Huang, H.; Liang, W.; et al. An overview of carbothermal synthesis of metal–biochar composites for the removal of oxyanion contaminants from aqueous solution. *Carbon* **2018**, *129*, 674–687. [[CrossRef](#)]
108. Vikrant, K.; Kim, K.-H.; Ok, Y.S.; Tsang, D.C.W.; Tsang, Y.F.; Giri, B.S.; Singh, R.S. Engineered/designer biochar for the removal of phosphate in water and wastewater. *Sci. Total Environ.* **2018**, *616*, 1242–1260. [[CrossRef](#)]
109. Bacelo, H.; Pintor, A.M.A.; Santos, S.C.R.; Boaventura, R.A.R.; Botelho, C.M.S. Performance and prospects of different adsorbents for phosphorus uptake and recovery from water. *Chem. Eng. J.* **2020**, *381*, 122566. [[CrossRef](#)]
110. Golterman, H. Natural phosphate sources in relation to phosphate budgets: A contribution to the understanding of eutrophication. *Phosphorus Fresh Water Mar. Environ. Prog. Water Technol.* **1973**, *2*, 3–17.
111. Smolders, A.; Lamers, L.; Lucassen, E.; Van der Velde, G.; Roelofs, J. Internal eutrophication: How it works and what to do about it—A review. *Chem. Ecol.* **2006**, *22*, 93–111. [[CrossRef](#)]
112. Correll, D.L. The role of phosphorus in the eutrophication of receiving waters: A review. *J. Environ. Qual.* **1998**, *27*, 261–266. [[CrossRef](#)]
113. Dieguez-Alonso, A.; Anca-Couce, A.; Frišták, V.; Moreno-Jiménez, E.; Bacher, M.; Bucheli, T.D.; Cimò, G.; Conte, P.; Hagemann, N.; Haller, A.; et al. Designing biochar properties through the blending of biomass feedstock with metals: Impact on oxyanions adsorption behavior. *Chemosphere* **2019**, *214*, 743–753. [[CrossRef](#)]
114. Trazzi, P.A.; Leahy, J.J.; Hayes, M.H.B.; Kwapinski, W. Adsorption and desorption of phosphate on biochars. *J. Environ. Chem. Eng.* **2016**, *4*, 37–46. [[CrossRef](#)]
115. Jung, K.-W.; Jeong, T.-U.; Kang, H.-J.; Chang, J.-S.; Ahn, K.-H. Preparation of modified-biochar from *Laminaria japonica*: Simultaneous optimization of aluminum electrode-based electro-modification and pyrolysis processes and its application for phosphate removal. *Bioresour. Technol.* **2016**, *214*, 548–557. [[CrossRef](#)] [[PubMed](#)]
116. Jung, K.-W.; Ahn, K.-H. Fabrication of porosity-enhanced MgO/biochar for removal of phosphate from aqueous solution: Application of a novel combined electrochemical modification method. *Bioresour. Technol.* **2016**, *200*, 1029–1032. [[CrossRef](#)] [[PubMed](#)]
117. Jung, K.-W.; Jeong, T.-U.; Hwang, M.-J.; Kim, K.; Ahn, K.-H. Phosphate adsorption ability of biochar/Mg–Al assembled nanocomposites prepared by aluminum-electrode based electro-assisted modification method with MgCl₂ as electrolyte. *Bioresour. Technol.* **2015**, *198*, 603–610. [[CrossRef](#)] [[PubMed](#)]
118. Jung, K.-W.; Jeong, T.-U.; Choi, J.-W.; Ahn, K.-H.; Lee, S.-H. Adsorption of phosphate from aqueous solution using electrochemically modified biochar calcium-alginate beads: Batch and fixed-bed column performance. *Bioresour. Technol.* **2017**, *244*, 23–32. [[CrossRef](#)] [[PubMed](#)]
119. Karydis, M. Eutrophication assessment of coastal waters based on indicators: A literature review. In Proceedings of the International Conference on Environmental Science and Technology, Mytilini, Greece, 4–7 September 2009.
120. Divband Hafshejani, L.; Hooshmand, A.; Naseri, A.A.; Mohammadi, A.S.; Abbasi, F.; Bhatnagar, A. Removal of nitrate from aqueous solution by modified sugarcane bagasse biochar. *Ecol. Eng.* **2016**, *95*, 101–111. [[CrossRef](#)]
121. Goswami, R.; Kumar, M. Removal of fluoride from aqueous solution using nanoscale rice husk biochar. *Groundw. Sustain. Dev.* **2018**, *7*, 446–451. [[CrossRef](#)]

122. Jin, J.; Li, S.; Peng, X.; Liu, W.; Zhang, C.; Yang, Y.; Han, L.; Du, Z.; Sun, K.; Wang, X. HNO₃ modified biochars for uranium (VI) removal from aqueous solution. *Bioresour. Technol.* **2018**, *256*, 247–253. [[CrossRef](#)]
123. Li, N.; Yin, M.; Tsang, D.C.W.; Yang, S.; Liu, J.; Li, X.; Song, G.; Wang, J. Mechanisms of U(VI) removal by biochar derived from *Ficus microcarpa* aerial root: A comparison between raw and modified biochar. *Sci. Total Environ.* **2019**, *697*, 134115. [[CrossRef](#)]
124. Harikishore Kumar Reddy, D.; Vijayaraghavan, K.; Kim, J.A.; Yun, Y.-S. Valorisation of post-sorption materials: Opportunities, strategies, and challenges. *Adv. Colloid Interface Sci.* **2017**, *242*, 35–58. [[CrossRef](#)]
125. Wang, L.; Wang, Y.; Ma, F.; Tankpa, V.; Bai, S.; Guo, X.; Wang, X. Mechanisms and reutilization of modified biochar used for removal of heavy metals from wastewater: A review. *Sci. Total Environ.* **2019**, *668*, 1298–1309. [[CrossRef](#)] [[PubMed](#)]
126. Hai, A.; Bharath, G.; Babu, K.R.; Taher, H.; Naushad, M.; Banat, F. Date seeds biomass-derived activated carbon for efficient removal of NaCl from saline solution. *Process Saf. Environ. Prot.* **2019**, *129*, 103–111. [[CrossRef](#)]
127. Welgemoed, T.; Schutte, C. Capacitive deionization technology™: An alternative desalination solution. *Desalination* **2005**, *183*, 327–340. [[CrossRef](#)]
128. Tang, Y.-H.; Liu, S.-H.; Tsang, D.C.W. Microwave-assisted production of CO₂-activated biochar from sugarcane bagasse for electrochemical desalination. *J. Hazard. Mater.* **2020**, *383*, 121192. [[CrossRef](#)] [[PubMed](#)]
129. Dehkoda, A.M.; Ellis, N.; Gyenge, E. Effect of activated biochar porous structure on the capacitive deionization of NaCl and ZnCl₂ solutions. *Microporous Mesoporous Mater.* **2016**, *224*, 217–228. [[CrossRef](#)]
130. Han, B.; Cheng, G.; Wang, Y.; Wang, X. Structure and functionality design of novel carbon and faradaic electrode materials for high-performance capacitive deionization. *Chem. Eng. J.* **2019**, *360*, 364–384. [[CrossRef](#)]
131. Meakins, N.; Bubb, J.; Lester, J. The fate and behaviour of organic micropollutants during wastewater treatment processes: A review. *Int. J. Environ. Pollut.* **1994**, *4*, 27–58.
132. Quesada, H.B.; Baptista, A.T.A.; Cusioli, L.F.; Seibert, D.; de Oliveira Bezerra, C.; Bergamasco, R. Surface water pollution by pharmaceuticals and an alternative of removal by low-cost adsorbents: A review. *Chemosphere* **2019**. [[CrossRef](#)]
133. Sharma, S.; Dutta, V.; Singh, P.; Raizada, P.; Rahmani-Sani, A.; Hosseini-Bandegharaei, A.; Thakur, V.K. Carbon quantum dot supported semiconductor photocatalysts for efficient degradation of organic pollutants in water: A review. *J. Clean. Prod.* **2019**. [[CrossRef](#)]
134. Ahmad, J.; Naeem, S.; Ahmad, M.; Usman, A.R.; Al-Wabel, M.I. A critical review on organic micropollutants contamination in wastewater and removal through carbon nanotubes. *J. Environ. Manag.* **2019**, *246*, 214–228. [[CrossRef](#)]
135. Baig, N.; Sajid, M.; Saleh, T.A. Graphene-based adsorbents for the removal of toxic organic pollutants: A review. *J. Environ. Manag.* **2019**, *244*, 370–382. [[CrossRef](#)] [[PubMed](#)]
136. Palansooriya, K.N.; Yang, Y.; Tsang, Y.F.; Sarkar, B.; Hou, D.; Cao, X.; Meers, E.; Rinklebe, J.; Kim, K.-H.; Ok, Y.S. Occurrence of contaminants in drinking water sources and the potential of biochar for water quality improvement: A review. *Crit. Rev. Environ. Sci. Technol.* **2019**, 1–63. [[CrossRef](#)]
137. Blanco-Canqui, H. Biochar and Water Quality. *J. Environ. Qual.* **2019**, *48*, 2–15. [[CrossRef](#)] [[PubMed](#)]
138. Tong, Y.; McNamara, P.J.; Mayer, B.K. Adsorption of organic micropollutants onto biochar: A review of relevant kinetics, mechanisms and equilibrium. *Environ. Sci. Water Res. Technol.* **2019**, *5*, 821–838. [[CrossRef](#)]
139. Peiris, C.; Gunatilake, S.R.; Mlsna, T.E.; Mohan, D.; Vithanage, M. Biochar based removal of antibiotic sulfonamides and tetracyclines in aquatic environments: A critical review. *Bioresour. Technol.* **2017**, *246*, 150–159. [[CrossRef](#)]
140. Sizmur, T.; Fresno, T.; Akgül, G.; Frost, H.; Moreno-Jiménez, E. Biochar modification to enhance sorption of inorganics from water. *Bioresour. Technol.* **2017**, *246*, 34–47. [[CrossRef](#)]
141. Premarathna, K.; Rajapaksha, A.U.; Sarkar, B.; Kwon, E.E.; Bhatnagar, A.; Ok, Y.S.; Vithanage, M. Biochar-based engineered composites for sorptive decontamination of water: A review. *Chem. Eng. J.* **2019**, *372*, 536–550. [[CrossRef](#)]

142. Bedia, J.; Peñas-Garzón, M.; Gómez-Avilés, A.; Rodríguez, J.J.; Belver, C. A review on the synthesis and characterization of biomass-derived carbons for adsorption of emerging contaminants from water. *C—J. Carbon Res.* **2018**, *4*, 63. [[CrossRef](#)]
143. Yu, Q.; Deng, S.; Yu, G. Selective removal of perfluorooctane sulfonate from aqueous solution using chitosan-based molecularly imprinted polymer adsorbents. *Water Res.* **2008**, *42*, 3089–3097. [[CrossRef](#)]
144. Dai, Y.; Zhang, N.; Xing, C.; Cui, Q.; Sun, Q. The adsorption, regeneration and engineering applications of biochar for removal organic pollutants: A review. *Chemosphere* **2019**, *223*, 12–27. [[CrossRef](#)]
145. Jayawardhana, Y.; Gunatilake, S.R.; Mahatantila, K.; Ginige, M.P.; Vithanage, M. Sorptive removal of toluene and m-xylene by municipal solid waste biochar: Simultaneous municipal solid waste management and remediation of volatile organic compounds. *J. Environ. Manag.* **2019**, *238*, 323–330. [[CrossRef](#)] [[PubMed](#)]
146. Kang, S.; Jung, J.; Choe, J.K.; Ok, Y.S.; Choi, Y. Effect of biochar particle size on hydrophobic organic compound sorption kinetics: Applicability of using representative size. *Sci. Total Environ.* **2018**, *619*, 410–418. [[CrossRef](#)] [[PubMed](#)]
147. Lingamdinne, L.P.; Roh, H.; Choi, Y.-L.; Koduru, J.R.; Yang, J.-K.; Chang, Y.-Y. Influencing factors on sorption of TNT and RDX using rice husk biochar. *J. Ind. Eng. Chem.* **2015**, *32*, 178–186. [[CrossRef](#)]
148. Mandal, S.; Sarkar, B.; Igalavithana, A.D.; Ok, Y.S.; Yang, X.; Lombi, E.; Bolan, N. Mechanistic insights of 2,4-D sorption onto biochar: Influence of feedstock materials and biochar properties. *Bioresour. Technol.* **2017**, *246*, 160–167. [[CrossRef](#)] [[PubMed](#)]
149. Zhu, L.; Zhao, N.; Tong, L.; Lv, Y.; Li, G. Characterization and evaluation of surface modified materials based on porous biochar and its adsorption properties for 2,4-dichlorophenoxyacetic acid. *Chemosphere* **2018**, *210*, 734–744. [[CrossRef](#)]
150. Silvani, L.; Cornelissen, G.; Hale, S.E. Sorption of α -, β -, γ - and δ -hexachlorocyclohexane isomers to three widely different biochars: Sorption mechanisms and application. *Chemosphere* **2019**, *219*, 1044–1051. [[CrossRef](#)]
151. AlAmeri, K.; Giwa, A.; Yousef, L.; Alraeesi, A.; Taher, H. Sorption and removal of crude oil spills from seawater using peat-derived biochar: An optimization study. *J. Environ. Manag.* **2019**, *250*, 109465. [[CrossRef](#)]
152. Robinson, T.; McMullan, G.; Marchant, R.; Nigam, P. Remediation of dyes in textile effluent: A critical review on current treatment technologies with a proposed alternative. *Bioresour. Technol.* **2001**, *77*, 247–255. [[CrossRef](#)]
153. Yagub, M.T.; Sen, T.K.; Afroze, S.; Ang, H.M. Dye and its removal from aqueous solution by adsorption: A review. *Adv. Colloid Interface Sci.* **2014**, *209*, 172–184. [[CrossRef](#)]
154. He, J.; Cui, A.; Deng, S.; Chen, J.P. Treatment of methylene blue containing wastewater by a cost-effective micro-scale biochar/polysulfone mixed matrix hollow fiber membrane: Performance and mechanism studies. *J. Colloid Interface Sci.* **2018**, *512*, 190–197. [[CrossRef](#)]
155. Hou, Y.; Huang, G.; Li, J.; Yang, Q.; Huang, S.; Cai, J. Hydrothermal conversion of bamboo shoot shell to biochar: Preliminary studies of adsorption equilibrium and kinetics for rhodamine B removal. *J. Anal. Appl. Pyrolysis* **2019**, *143*, 104694. [[CrossRef](#)]
156. Zhang, Z.; O'Hara, I.M.; Kent, G.A.; Doherty, W.O.S. Comparative study on adsorption of two cationic dyes by milled sugarcane bagasse. *Ind. Crop. Prod.* **2013**, *42*, 41–49. [[CrossRef](#)]
157. Zazycki, M.A.; Godinho, M.; Perondi, D.; Foletto, E.L.; Collazzo, G.C.; Dotto, G.L. New biochar from pecan nutshells as an alternative adsorbent for removing reactive red 141 from aqueous solutions. *J. Clean. Prod.* **2018**, *171*, 57–65. [[CrossRef](#)]
158. Netpradit, S.; Thiravetyan, P.; Towprayoon, S. Application of 'waste' metal hydroxide sludge for adsorption of azo reactive dyes. *Water Res.* **2003**, *37*, 763–772. [[CrossRef](#)]
159. Jung, K.-W.; Choi, B.H.; Jeong, T.-U.; Ahn, K.-H. Facile synthesis of magnetic biochar/Fe₃O₄ nanocomposites using electro-magnetization technique and its application on the removal of acid orange 7 from aqueous media. *Bioresour. Technol.* **2016**, *220*, 672–676. [[CrossRef](#)]
160. Yoon, S.; Calvo, J.; So, M. Removal of Acid Orange 7 from Aqueous Solution by Metal-Organic Frameworks. *Crystals* **2019**, *9*, 17. [[CrossRef](#)]

161. Heo, J.; Yoon, Y.; Lee, G.; Kim, Y.; Han, J.; Park, C.M. Enhanced adsorption of bisphenol A and sulfamethoxazole by a novel magnetic CuZnFe₂O₄-biochar composite. *Bioresour. Technol.* **2019**, *281*, 179–187. [[CrossRef](#)]
162. Wang, D.; Sui, Q.; Zhao, W.; Shuguang, L.; Qiu, Z.; Yu, G. Pharmaceutical and personal care products in the surface water of China: A review. *Chin. Sci. Bull.* **2014**, *59*, 743–751.
163. Derksen, J.; Rijs, G.; Jongbloed, R. Diffuse pollution of surface water by pharmaceutical products. *Water Sci. Technol.* **2004**, *49*, 213–221. [[CrossRef](#)]
164. Larsson, D.J. Pollution from drug manufacturing: Review and perspectives. *Philos. Trans. R. Soc. B Biol. Sci.* **2014**, *369*, 20130571. [[CrossRef](#)]
165. Kim, S.; Park, C.M.; Jang, A.; Jang, M.; Hernández-Maldonado, A.J.; Yu, M.; Heo, J.; Yoon, Y. Removal of selected pharmaceuticals in an ultrafiltration-activated biochar hybrid system. *J. Membr. Sci.* **2019**, *570*, 77–84. [[CrossRef](#)]
166. Li, F.; Feng, D.; Deng, H.; Yu, H.; Ge, C. Effects of Biochars Prepared from Cassava Dregs on Sorption Behavior of Ciprofloxacin. *Procedia Environ. Sci.* **2016**, *31*, 795–803. [[CrossRef](#)]
167. Jang, H.M.; Kan, E. Engineered biochar from agricultural waste for removal of tetracycline in water. *Bioresour. Technol.* **2019**, *284*, 437–447. [[CrossRef](#)] [[PubMed](#)]
168. Mandal, A.; Singh, N. Optimization of atrazine and imidacloprid removal from water using biochars: Designing single or multi-staged batch adsorption systems. *Int. J. Hyg. Environ. Health* **2017**, *220*, 637–645. [[CrossRef](#)]
169. Xu, J.; Cao, Z.; Wang, Y.; Zhang, Y.; Gao, X.; Ahmed, M.B.; Zhang, J.; Yang, Y.; Zhou, J.L.; Lowry, G.V. Distributing sulfidized nanoscale zerovalent iron onto phosphorus-functionalized biochar for enhanced removal of antibiotic florfenicol. *Chem. Eng. J.* **2019**, *359*, 713–722. [[CrossRef](#)]
170. Zhang, M.-h.; Dong, H.; Zhao, L.; Wang, D.-X.; Meng, D. A review on Fenton process for organic wastewater treatment based on optimization perspective. *Sci. Total Environ.* **2019**. [[CrossRef](#)]
171. Matzek, L.W.; Carter, K.E. Activated persulfate for organic chemical degradation: A review. *Chemosphere* **2016**, *151*, 178–188. [[CrossRef](#)]
172. Huang, D.; Luo, H.; Zhang, C.; Zeng, G.; Lai, C.; Cheng, M.; Wang, R.; Deng, R.; Xue, W.; Gong, X.; et al. Nonnegligible role of biomass types and its compositions on the formation of persistent free radicals in biochar: Insight into the influences on Fenton-like process. *Chem. Eng. J.* **2019**, *361*, 353–363. [[CrossRef](#)]
173. He, J.; Xiao, Y.; Tang, J.; Chen, H.; Sun, H. Persulfate activation with sawdust biochar in aqueous solution by enhanced electron donor-transfer effect. *Sci. Total Environ.* **2019**, *690*, 768–777. [[CrossRef](#)]
174. Ho, S.-H.; Chen, Y.-d.; Li, R.; Zhang, C.; Ge, Y.; Cao, G.; Ma, M.; Duan, X.; Wang, S.; Ren, N.-Q. N-doped graphitic biochars from C-phycoyanin extracted Spirulina residue for catalytic persulfate activation toward nonradical disinfection and organic oxidation. *Water Res.* **2019**, *159*, 77–86. [[CrossRef](#)]
175. Fu, H.; Zhao, P.; Xu, S.; Cheng, G.; Li, Z.; Li, Y.; Li, K.; Ma, S. Fabrication of Fe₃O₄ and graphitized porous biochar composites for activating peroxymonosulfate to degrade p-hydroxybenzoic acid: Insights on the mechanism. *Chem. Eng. J.* **2019**, *375*, 121980. [[CrossRef](#)]
176. Dong, C.-D.; Chen, C.-W.; Tsai, M.-L.; Chang, J.-H.; Lyu, S.-Y.; Hung, C.-M. Degradation of 4-nonylphenol in marine sediments by persulfate over magnetically modified biochars. *Bioresour. Technol.* **2019**, *281*, 143–148. [[CrossRef](#)] [[PubMed](#)]
177. Liu, C.; Chen, L.; Ding, D.; Cai, T. From rice straw to magnetically recoverable nitrogen doped biochar: Efficient activation of peroxymonosulfate for the degradation of metolachlor. *Appl. Catal. B: Environ.* **2019**, *254*, 312–320. [[CrossRef](#)]
178. Jiang, S.-F.; Ling, L.-L.; Chen, W.-J.; Liu, W.-J.; Li, D.-C.; Jiang, H. High efficient removal of bisphenol A in a peroxymonosulfate/iron functionalized biochar system: Mechanistic elucidation and quantification of the contributors. *Chem. Eng. J.* **2019**, *359*, 572–583. [[CrossRef](#)]
179. Jung, K.-W.; Lee, S.Y.; Lee, Y.J.; Choi, J.-W. Ultrasound-assisted heterogeneous Fenton-like process for bisphenol A removal at neutral pH using hierarchically structured manganese dioxide/biochar nanocomposites as catalysts. *Ultrason. Sonochem.* **2019**, *57*, 22–28. [[CrossRef](#)]

180. Diao, Z.-H.; Dong, F.-X.; Yan, L.; Chen, Z.-L.; Qian, W.; Kong, L.-J.; Zhang, Z.-W.; Zhang, T.; Tao, X.-Q.; Du, J.-J.; et al. Synergistic oxidation of Bisphenol A in a heterogeneous ultrasound-enhanced sludge biochar catalyst/persulfate process: Reactivity and mechanism. *J. Hazard. Mater.* **2019**. [[CrossRef](#)]
181. Gan, L.; Zhong, Q.; Geng, A.; Wang, L.; Song, C.; Han, S.; Cui, J.; Xu, L. Cellulose derived carbon nanofiber: A promising biochar support to enhance the catalytic performance of CoFe₂O₄ in activating peroxydisulfate for recycled dimethyl phthalate degradation. *Sci. Total Environ.* **2019**, *694*, 133705. [[CrossRef](#)]
182. Moussavi, G.; Khosravi, R. Preparation and characterization of a biochar from pistachio hull biomass and its catalytic potential for ozonation of water recalcitrant contaminants. *Bioresour. Technol.* **2012**, *119*, 66–71. [[CrossRef](#)]
183. Oh, S.-Y.; Seo, Y.-D.; Ryu, K.-S. Reductive removal of 2,4-dinitrotoluene and 2,4-dichlorophenol with zero-valent iron-included biochar. *Bioresour. Technol.* **2016**, *216*, 1014–1021. [[CrossRef](#)]
184. Zhang, D.; Li, Y.; Sun, A.; Tong, S.; Su, G.; Jiang, X.; Li, J.; Han, W.; Sun, X.; Wang, L.; et al. Enhanced nitrobenzene reduction by modified biochar supported sulfidated nano zerovalent iron: Comparison of surface modification methods. *Sci. Total Environ.* **2019**, *694*, 133701. [[CrossRef](#)]
185. Lyu, H.; Tang, J.; Shen, B.; Siddique, T. Development of a novel chem-bio hybrid process using biochar supported nanoscale iron sulfide composite and *Corynebacterium variabile* HRJ4 for enhanced trichloroethylene dechlorination. *Water Res.* **2018**, *147*, 132–141. [[CrossRef](#)] [[PubMed](#)]
186. Sophia Ayyappan, C.; Bhalambaal, V.M.; Kumar, S. Effect of biochar on bio-electrochemical dye degradation and energy production. *Bioresour. Technol.* **2018**, *251*, 165–170. [[CrossRef](#)] [[PubMed](#)]
187. Chong, M.N.; Jin, B.; Chow, C.W.; Saint, C. Recent developments in photocatalytic water treatment technology: A review. *Water Res.* **2010**, *44*, 2997–3027. [[CrossRef](#)] [[PubMed](#)]
188. Shirvanimoghaddam, K.; Czech, B.; Wójcik, G.; Naebe, M. The light enhanced removal of Bisphenol A from wastewater using cotton waste derived carbon microtubes. *J. Colloid Interface Sci.* **2019**, *539*, 425–432. [[CrossRef](#)] [[PubMed](#)]
189. Li, S.; Wang, Z.; Zhao, X.; Yang, X.; Liang, G.; Xie, X. Insight into enhanced carbamazepine photodegradation over biochar-based magnetic photocatalyst Fe₃O₄/BiOBr/BC under visible LED light irradiation. *Chem. Eng. J.* **2019**, *360*, 600–611. [[CrossRef](#)]
190. Kumar, A.; Kumar, A.; Sharma, G.; Al-Muhtaseb, A.a.H.; Naushad, M.; Ghfar, A.A.; Guo, C.; Stadler, F.J. Biochar-templated g-C₃N₄/Bi₂O₂CO₃/CoFe₂O₄ nano-assembly for visible and solar assisted photo-degradation of paraquat, nitrophenol reduction and CO₂ conversion. *Chem. Eng. J.* **2018**, *339*, 393–410. [[CrossRef](#)]
191. Kumar, A.; Sharma, G.; Naushad, M.; Al-Muhtaseb, A.a.H.; Kumar, A.; Hira, I.; Ahamad, T.; Ghfar, A.A.; Stadler, F.J. Visible photodegradation of ibuprofen and 2,4-D in simulated waste water using sustainable metal free-hybrids based on carbon nitride and biochar. *J. Environ. Manag.* **2019**, *231*, 1164–1175. [[CrossRef](#)]
192. Xie, X.; Li, S.; Zhang, H.; Wang, Z.; Huang, H. Promoting charge separation of biochar-based Zn-TiO₂/pBC in the presence of ZnO for efficient sulfamethoxazole photodegradation under visible light irradiation. *Sci. Total Environ.* **2019**, *659*, 529–539. [[CrossRef](#)]
193. Kohl, A.L.; Nielsen, R. *Gas Purification*; Elsevier: Amsterdam, The Netherlands, 1997.
194. Eddaoudi, M.; Almaythaly, B.A.; Shekha, O.; Belmabkhout, Y. Zeolite-Like Metal-Organic Framework Membrane. U.S. Patent US10130908B2, 20 November 2018.
195. Kimura, S.; Walmet, G. Fuel gas purification with permselective membranes. *Sep. Sci. Technol.* **1980**, *15*, 1115–1133. [[CrossRef](#)]
196. Dumée, L.; Scholes, C.; Stevens, G.; Kentish, S. Purification of aqueous amine solvents used in post combustion CO₂ capture: A review. *Int. J. Greenh. Gas Control* **2012**, *10*, 443–455. [[CrossRef](#)]
197. Das, J.; Rene, E.R.; Dupont, C.; Dufourny, A.; Blin, J.; van Hullebusch, E.D. Performance of a compost and biochar packed biofilter for gas-phase hydrogen sulfide removal. *Bioresour. Technol.* **2019**, *273*, 581–591. [[CrossRef](#)] [[PubMed](#)]
198. Braghiroli, F.L.; Bouafif, H.; Koubaa, A. Enhanced SO₂ adsorption and desorption on chemically and physically activated biochar made from wood residues. *Ind. Crop. Prod.* **2019**, *138*, 111456. [[CrossRef](#)]
199. Shao, J.; Zhang, J.; Zhang, X.; Feng, Y.; Zhang, H.; Zhang, S.; Chen, H. Enhance SO₂ adsorption performance of biochar modified by CO₂ activation and amine impregnation. *Fuel* **2018**, *224*, 138–146. [[CrossRef](#)]
200. Rind, D.; Suozzo, R.; Balachandran, N.; Prather, M. Climate change and the middle atmosphere. Part I: The doubled CO₂ climate. *J. Atmos. Sci.* **1990**, *47*, 475–494. [[CrossRef](#)]

201. Feijoo, F.; Mignone, B.K.; Khesghi, H.S.; Hartin, C.; McJeon, H.; Edmonds, J. Climate and carbon budget implications of linked future changes in CO₂ and non-CO₂ forcing. *Environ. Res. Lett.* **2019**, *14*, 044007. [[CrossRef](#)]
202. Kellogg, W.W. *Climate Change and Society: Consequences of Increasing Atmospheric Carbon Dioxide*; Routledge: Abingdon upon Thames, UK, 2019.
203. Jung, S.; Park, Y.-K.; Kwon, E.E. Strategic use of biochar for CO₂ capture and sequestration. *J. CO₂ Util.* **2019**, *32*, 128–139. [[CrossRef](#)]
204. Liu, S.-H.; Huang, Y.-Y. Valorization of coffee grounds to biochar-derived adsorbents for CO₂ adsorption. *J. Clean. Prod.* **2018**, *175*, 354–360. [[CrossRef](#)]
205. Igalavithana, A.D.; Choi, S.W.; Dissanayake, P.D.; Shang, J.; Wang, C.-H.; Yang, X.; Kim, S.; Tsang, D.C.; Lee, K.B.; Ok, Y.S. Gasification biochar from biowaste (food waste and wood waste) for effective CO₂ adsorption. *J. Hazard. Mater.* **2019**, 121147. [[CrossRef](#)]
206. Huang, Y.-F.; Chiueh, P.-T.; Lo, S.-L. CO₂ adsorption on biochar from co-torrefaction of sewage sludge and leucaena wood using microwave heating. *Energy Procedia* **2019**, *158*, 4435–4440. [[CrossRef](#)]
207. Chiang, Y.-C.; Juang, R.-S. Surface modifications of carbonaceous materials for carbon dioxide adsorption: A review. *J. Taiwan Inst. Chem. Eng.* **2017**, *71*, 214–234. [[CrossRef](#)]
208. Zhang, X.; Zhang, S.; Yang, H.; Shao, J.; Chen, Y.; Feng, Y.; Wang, X.; Chen, H. Effects of hydrofluoric acid pre-leaching of rice husk on physicochemical properties and CO₂ adsorption performance of nitrogen-enriched biochar. *Energy* **2015**, *91*, 903–910. [[CrossRef](#)]
209. Huang, Y.-F.; Chiueh, P.-T.; Shih, C.-H.; Lo, S.-L.; Sun, L.; Zhong, Y.; Qiu, C. Microwave pyrolysis of rice straw to produce biochar as an adsorbent for CO₂ capture. *Energy* **2015**, *84*, 75–82. [[CrossRef](#)]
210. Shen, Y.; Fu, Y. KOH-activated rice husk char via CO₂ pyrolysis for phenol adsorption. *Mater. Today Energy* **2018**, *9*, 397–405. [[CrossRef](#)]
211. Przepiórski, J.; Skrodzewicz, M.; Morawski, A. High temperature ammonia treatment of activated carbon for enhancement of CO₂ adsorption. *Appl. Surf. Sci.* **2004**, *225*, 235–242. [[CrossRef](#)]
212. Shafeeyan, M.S.; Daud, W.M.A.W.; Houshmand, A.; Arami-Niya, A. Ammonia modification of activated carbon to enhance carbon dioxide adsorption: Effect of pre-oxidation. *Appl. Surf. Sci.* **2011**, *257*, 3936–3942. [[CrossRef](#)]
213. Xie, P.; Sun, F.; Wang, L.; Liu, P. A review on China's Energy Storage Industry under the "Internet Plus" initiative. *Int. J. Energy Res.* **2019**, *43*, 717–741. [[CrossRef](#)]
214. Winter, M.; Brodd, R.J. *What are Batteries, Fuel Cells, and Supercapacitors*; ACS Publications: Washington, DC, USA, 2004.
215. Fonash, S. *Solar Cell Device Physics*; Elsevier: Amsterdam, The Netherlands, 2012.
216. Blomen, L.J.; Mugerwa, M.N. *Fuel Cell Systems*; Springer Science & Business Media: Berlin, Germany, 2013.
217. Yoshio, M.; Brodd, R.J.; Kozawa, A. *Lithium-Ion Batteries*; Springer: Berlin, Germany, 2009; Volume 1.
218. Lu, M. *Supercapacitors: Materials, Systems and Applications*; John Wiley & Sons: Hoboken, NJ, USA, 2013.
219. Winter, M.; Brodd, R.J. What Are Batteries, Fuel Cells, and Supercapacitors? *Chem. Rev.* **2004**, *104*, 4245–4270. [[CrossRef](#)]
220. Etacheri, V.; Marom, R.; Elazari, R.; Salitra, G.; Aurbach, D. Challenges in the development of advanced Li-ion batteries: A review. *Energy Environ. Sci.* **2011**, *4*, 3243–3262. [[CrossRef](#)]
221. Kubota, K.; Komaba, S. practical issues and future perspective for Na-ion batteries. *J. Electrochem. Soc.* **2015**, *162*, A2538–A2550. [[CrossRef](#)]
222. Dodds, P.E.; Staffell, I.; Hawkes, A.D.; Li, F.; Grünewald, P.; McDowall, W.; Ekins, P. Hydrogen and fuel cell technologies for heating: A review. *Int. J. Hydrog. Energy* **2015**, *40*, 2065–2083. [[CrossRef](#)]
223. Giddey, S.; Badwal, S.; Kulkarni, A.; Munnings, C. A comprehensive review of direct carbon fuel cell technology. *Prog. Energy Combust. Sci.* **2012**, *38*, 360–399. [[CrossRef](#)]
224. Munjewar, S.S.; Thombre, S.B.; Mallick, R.K. Approaches to overcome the barrier issues of passive direct methanol fuel cell—Review. *Renew. Sustain. Energy Rev.* **2017**, *67*, 1087–1104. [[CrossRef](#)]
225. Bartoli, M.; Rosi, L.; Frediani, M.; Frediani, P. *Challenges and Opportunities in the Field of Energy Storage: Supercapacitors and Activated Biochar*; Nova Publisher: Hauppauge, NY, USA, 2018.
226. Jin, H.; Wang, X.; Gu, Z.; Polin, J. Carbon materials from high ash biochar for supercapacitor and improvement of capacitance with HNO₃ surface oxidation. *J. Power Sources* **2013**, *236*, 285–292. [[CrossRef](#)]

227. Gabhi, R.S.; Kirk, D.W.; Jia, C.Q. Preliminary investigation of electrical conductivity of monolithic biochar. *Carbon* **2017**, *116*, 435–442. [[CrossRef](#)]
228. Luo, W.; Wang, B.; Heron, C.G.; Allen, M.J.; Morre, J.; Maier, C.S.; Stickle, W.F.; Ji, X. Pyrolysis of cellulose under ammonia leads to nitrogen-doped nanoporous carbon generated through methane formation. *Nano Lett.* **2014**, *14*, 2225–2229. [[CrossRef](#)]
229. Qu, W.-H.; Xu, Y.-Y.; Lu, A.-H.; Zhang, X.-Q.; Li, W.-C. Converting biowaste corncob residue into high value added porous carbon for supercapacitor electrodes. *Bioresour. Technol.* **2015**, *189*, 285–291. [[CrossRef](#)]
230. Cheng, B.-H.; Tian, K.; Zeng, R.J.; Jiang, H. Preparation of high performance supercapacitor materials by fast pyrolysis of corn gluten meal waste. *Sustain. Energy Fuels* **2017**, *1*, 891–898. [[CrossRef](#)]
231. Sun, W.; Lipka, S.M.; Swartz, C.; Williams, D.; Yang, F. Hemp-derived activated carbons for supercapacitors. *Carbon* **2016**, *103*, 181–192. [[CrossRef](#)]
232. Sivachidambaram, M.; Vijaya, J.J.; Kennedy, L.J.; Jothiramalingam, R.; Al-Lohedan, H.A.; Munusamy, M.A.; Elanthamilan, E.; Merlin, J.P. Preparation and characterization of activated carbon derived from the *Borassus flabellifer* flower as an electrode material for supercapacitor applications. *New J. Chem.* **2017**, *41*, 3939–3949. [[CrossRef](#)]
233. Zou, R.; Quan, H.; Wang, W.; Gao, W.; Dong, Y.; Chen, D. Porous carbon with interpenetrating framework from *Osmanthus* flower as electrode materials for high-performance supercapacitor. *J. Environ. Chem. Eng.* **2018**, *6*, 258–265. [[CrossRef](#)]
234. Song, M.; Zhou, Y.; Ren, X.; Wan, J.; Du, Y.; Wu, G.; Ma, F. Biowaste-based porous carbon for supercapacitor: The influence of preparation processes on structure and performance. *J. Colloid Interface Sci.* **2019**, *535*, 276–286. [[CrossRef](#)] [[PubMed](#)]
235. Zhang, Y.; Sun, C.; Tang, Z. High specific capacitance and high energy density supercapacitor electrodes enabled by porous carbon with multilevel pores and self-doped heteroatoms derived from Chinese date. *Diam. Relat. Mater.* **2019**, *97*, 107455. [[CrossRef](#)]
236. Zhang, Y.-L.; Li, S.-Y.; Tang, Z.-S.; Song, Z.-X.; Sun, J. Xanthoceras sorbifolia seed coats derived porous carbon with unique architecture for high rate performance supercapacitors. *Diam. Relat. Mater.* **2019**, *91*, 119–126. [[CrossRef](#)]
237. Jiao, C.; Xu, J.L.; Chen, X.Y.; Zhang, Z.J. Design and synthesis of phosphomolybdic acid/silver dual-modified microporous carbon composite for high performance supercapacitors. *J. Alloy. Compd.* **2019**, *791*, 1005–1014. [[CrossRef](#)]
238. Gupta, R.K.; Dubey, M.; Kharel, P.; Gu, Z.; Fan, Q.H. Biochar activated by oxygen plasma for supercapacitors. *J. Power Sources* **2015**, *274*, 1300–1305. [[CrossRef](#)]
239. Gao, Y.; Xu, S.; Yue, Q.; Ortaboy, S.; Gao, B.; Sun, Y. Synthesis and characterization of heteroatom-enriched biochar from keratin-based and algous-based wastes. *Adv. Powder Technol.* **2016**, *27*, 1280–1286. [[CrossRef](#)]
240. Pontiroli, D.; Scaravonati, S.; Magnani, G.; Fornasini, L.; Bersani, D.; Bertoni, G.; Milanese, C.; Girella, A.; Ridi, F.; Verucchi, R.; et al. Super-activated biochar from poultry litter for high-performance supercapacitors. *Microporous Mesoporous Mater.* **2019**, *285*, 161–169. [[CrossRef](#)]
241. Dai, X.-H.; Fan, H.-X.; Zhang, J.-J.; Yuan, S.-J. Sewage sludge-derived porous hollow carbon nanospheres as high-performance anode material for lithium ion batteries. *Electrochim. Acta* **2019**, *319*, 277–285. [[CrossRef](#)]
242. Luna-Lama, F.; Rodríguez-Padrón, D.; Puente-Santiago, A.R.; Muñoz-Batista, M.J.; Caballero, A.; Balu, A.M.; Romero, A.A.; Luque, R. Non-porous carbonaceous materials derived from coffee waste grounds as highly sustainable anodes for lithium-ion batteries. *J. Clean. Prod.* **2019**, *207*, 411–417. [[CrossRef](#)]
243. Zhang, H.; Yu, F.; Kang, W.; Shen, Q. Encapsulating selenium into macro-/micro-porous biochar-based framework for high-performance lithium-selenium batteries. *Carbon* **2015**, *95*, 354–363. [[CrossRef](#)]
244. Benítez, A.; González-Tejero, M.; Caballero, Á.; Morales, J. Almond Shell as a Microporous Carbon Source for Sustainable Cathodes in Lithium–Sulfur Batteries. *Materials* **2018**, *11*, 1428. [[CrossRef](#)]
245. Chen, X.; Du, G.; Zhang, M.; Kalam, A.; Su, Q.; Ding, S.; Xu, B. Nitrogen-doped hierarchical porous carbon derived from low-cost biomass pomegranate residues for high performance lithium-sulfur batteries. *J. Electroanal. Chem.* **2019**, *848*, 113316. [[CrossRef](#)]
246. Chen, F.; Ma, L.; Ren, J.; Zhang, M.; Luo, X.; Li, B.; Song, Z.; Zhou, X. Wheat Straw-Derived N-, O-, and S-Tri-doped Porous Carbon with Ultrahigh Specific Surface Area for Lithium-Sulfur Batteries. *Materials* **2018**, *11*, 989. [[CrossRef](#)] [[PubMed](#)]

247. Magnacca, G.; Guerretta, F.; Vizintin, A.; Benzi, P.; Valsania, M.C.; Nisticò, R. Preparation, characterization and environmental/electrochemical energy storage testing of low-cost biochar from natural chitin obtained via pyrolysis at mild conditions. *Appl. Surf. Sci.* **2018**, *427*, 883–893. [[CrossRef](#)]
248. Pan, P.; Hu, Y.; Wu, K.; Cheng, Z.; Shen, Z.; Jiang, L.; Mao, J.; Ni, C.; Ge, Y.; Wang, Z. Growth of ZnCo₂O₄ nanocubes on flexible biochar substrate derived from natural silk waste fabric for lithium-ion battery anode. *J. Alloy. Compd.* **2020**, *814*, 152306. [[CrossRef](#)]
249. Li, T.; Bai, X.; Qi, Y.-X.; Lun, N.; Bai, Y.-J. Fe₃O₄ nanoparticles decorated on the biochar derived from pomelo pericarp as excellent anode materials for Li-ion batteries. *Electrochim. Acta* **2016**, *222*, 1562–1568. [[CrossRef](#)]
250. Salimi, P.; Norouzi, O.; Pourhoseini, S.E.M.; Bartocci, P.; Tavasoli, A.; Di Maria, F.; Pirbazari, S.M.; Bidini, G.; Fantozzi, F. Magnetic biochar obtained through catalytic pyrolysis of macroalgae: A promising anode material for Li-ion batteries. *Renew. Energy* **2019**, *140*, 704–714. [[CrossRef](#)]
251. Salimi, P.; Norouzi, O.; Pourhosseini, S.E.M. Two-step synthesis of nanohusk Fe₃O₄ embedded in 3D network pyrolytic marine biochar for a new generation of anode materials for Lithium-Ion batteries. *J. Alloy. Compd.* **2019**, *786*, 930–937. [[CrossRef](#)]
252. Saavedra Rios, C.d.M.; Simone, V.; Simonin, L.; Martinet, S.; Dupont, C. Biochars from various biomass types as precursors for hard carbon anodes in sodium-ion batteries. *Biomass Bioenergy* **2018**, *117*, 32–37. [[CrossRef](#)]
253. Jafri, N.; Wong, W.Y.; Doshi, V.; Yoon, L.W.; Cheah, K.H. A review on production and characterization of biochars for application in direct carbon fuel cells. *Process Saf. Environ. Prot.* **2018**, *118*, 152–166. [[CrossRef](#)]
254. Konsolakis, M.; Kaklidis, N.; Marnellos, G.E.; Zaharaki, D.; Komnitsas, K. Assessment of biochar as feedstock in a direct carbon solid oxide fuel cell. *RSC Adv.* **2015**, *5*, 73399–73409. [[CrossRef](#)]
255. Elleuch, A.; Halouani, K.; Li, Y. Investigation of chemical and electrochemical reactions mechanisms in a direct carbon fuel cell using olive wood charcoal as sustainable fuel. *J. Power Sources* **2015**, *281*, 350–361. [[CrossRef](#)]
256. Xu, K.; Dong, J.; Li, X.; Wang, J.; Hu, Z.; Li, A.; Yao, H. Evaluation of biomass and its thermal decomposition products as fuels for direct carbon fuel cells. *Biomass Bioenergy* **2019**, *130*, 105359. [[CrossRef](#)]
257. Qiu, Q.; Zhou, M.; Cai, W.; Zhou, Q.; Zhang, Y.; Wang, W.; Liu, M.; Liu, J. A comparative investigation on direct carbon solid oxide fuel cells operated with fuels of biochar derived from wheat straw, corncob, and bagasse. *Biomass Bioenergy* **2019**, *121*, 56–63. [[CrossRef](#)]
258. Kacprzak, A.; Kobylecki, R.; Włodarczyk, R.; Bis, Z. The effect of fuel type on the performance of a direct carbon fuel cell with molten alkaline electrolyte. *J. Power Sources* **2014**, *255*, 179–186. [[CrossRef](#)]
259. Kacprzak, A.; Kobylecki, R.; Włodarczyk, R.; Bis, Z. Efficiency of non-optimized direct carbon fuel cell with molten alkaline electrolyte fueled by carbonized biomass. *J. Power Sources* **2016**, *321*, 233–240. [[CrossRef](#)]
260. Kacprzak, A.; Kobylecki, R.; Bis, Z. Influence of temperature and composition of NaOH–KOH and NaOH–LiOH electrolytes on the performance of a direct carbon fuel cell. *J. Power Sources* **2013**, *239*, 409–414. [[CrossRef](#)]
261. Ali, A.; Raza, R.; Shakir, M.I.; Iftikhar, A.; Alvi, F.; Ullah, M.K.; Hamid, A.; Kim, J.-S. Promising electrochemical study of titanate based anodes in direct carbon fuel cell using walnut and almond shells biochar fuel. *J. Power Sources* **2019**, *434*, 126679. [[CrossRef](#)]
262. Elleuch, A.; Boussetta, A.; Yu, J.; Halouani, K.; Li, Y. Experimental investigation of direct carbon fuel cell fueled by almond shell biochar: Part I. Physico-chemical characterization of the biochar fuel and cell performance examination. *Int. J. Hydrog. Energy* **2013**, *38*, 16590–16604. [[CrossRef](#)]
263. Huggins, T.; Wang, H.; Kearns, J.; Jenkins, P.; Ren, Z.J. Biochar as a sustainable electrode material for electricity production in microbial fuel cells. *Bioresour. Technol.* **2014**, *157*, 114–119. [[CrossRef](#)]
264. Huggins, T.M.; Pietron, J.J.; Wang, H.; Ren, Z.J.; Biffinger, J.C. Graphitic biochar as a cathode electrocatalyst support for microbial fuel cells. *Bioresour. Technol.* **2015**, *195*, 147–153. [[CrossRef](#)]
265. Md Khudzari, J.; Gariépy, Y.; Kurian, J.; Tartakovsky, B.; Raghavan, G.S.V. Effects of biochar anodes in rice plant microbial fuel cells on the production of bioelectricity, biomass, and methane. *Biochem. Eng. J.* **2019**, *141*, 190–199. [[CrossRef](#)]
266. Li, M.; Zhang, H.; Xiao, T.; Wang, S.; Zhang, B.; Chen, D.; Su, M.; Tang, J. Low-cost biochar derived from corncob as oxygen reduction catalyst in air cathode microbial fuel cells. *Electrochim. Acta* **2018**, *283*, 780–788. [[CrossRef](#)]
267. Yuan, Y.; Yuan, T.; Wang, D.; Tang, J.; Zhou, S. Sewage sludge biochar as an efficient catalyst for oxygen reduction reaction in a microbial fuel cell. *Bioresour. Technol.* **2013**, *144*, 115–120. [[CrossRef](#)]

268. Chakraborty, I.; Das, S.; Dubey, B.K.; Ghangrekar, M.M. Novel low cost proton exchange membrane made from sulphonated biochar for application in microbial fuel cells. *Mater. Chem. Phys.* **2020**, *239*, 122025. [CrossRef]
269. Research, G.V. Market Value of Composite Materials Worldwide from 2015 to 2024 (in Billion U.S. Dollars). Available online: <https://www.statista.com/statistics/944471/global-market-value-of-composites/> (accessed on 3 November 2019).
270. Sauer, M.; Kühnel, M.; Witten, E. *Composites Market Report 2018—Market Developments, Trends, Outlook and Challenges*; AVK-TV Industrievereinigung verstärkte Kunststoffe Carbon Composite: Augsburg, Germany, 2018.
271. Chand, S. Review carbon fibers for composites. *J. Mater. Sci.* **2000**, *35*, 1303–1313. [CrossRef]
272. Samal, S.S.; Bal, S. Carbon nanotube reinforced ceramic matrix composites—a review. *J. Miner. Mater. Charact. Eng.* **2008**, *7*, 355. [CrossRef]
273. Afzal, A.; Kausar, A.; Siddiq, M. A review on polymer/cement composite with carbon nanofiller and inorganic filler. *Polym. Plast. Technol. Eng.* **2016**, *55*, 1299–1323. [CrossRef]
274. Downie, A.; Crosky, A.; Munroe, P. Physical properties of biochar. *Biochar Environ. Manag. Sci. Technol.* **2009**, *2*, 13–32.
275. Bernhardt, D.; Reilly, J., II. *Mineral Commodity Summaries 2019*; Department of the Interior (DOI), U.S. Geological Survey (USGS): Reston, VA, USA, 2019.
276. Lewis, S.J.; Sodhi, T.S.; Agapiou, K.; Kolasnikov, A. Non-Aqueous Liquid Anti-Shrinkage Cement Additives. U.S. Patents US20190062213A1, 28 February 2019.
277. Riley, V.; Razl, I. Polymer additives for cement composites: A review. *Composites* **1974**, *5*, 27–33. [CrossRef]
278. Reales, O.A.M.; Toledo Filho, R.D. A review on the chemical, mechanical and microstructural characterization of carbon nanotubes-cement based composites. *Constr. Build. Mater.* **2017**, *154*, 697–710. [CrossRef]
279. Yang, H.; Cui, H.; Tang, W.; Li, Z.; Han, N.; Xing, F. A critical review on research progress of graphene/cement based composites. *Compos. Part A Appl. Sci. Manuf.* **2017**, *102*, 273–296. [CrossRef]
280. Toutanji, H.A.; El-Korchi, T.; Katz, R.N. Strength and reliability of carbon-fiber-reinforced cement composites. *Cem. Concr. Compos.* **1994**, *16*, 15–21. [CrossRef]
281. Cosentino, I.; Restuccia, L.; Ferro, G.A.; Tulliani, J.-M. Type of materials, pyrolysis conditions, carbon content and size dimensions: The parameters that influence the mechanical properties of biochar cement-based composites. *Theor. Appl. Fract. Mech.* **2019**, *103*, 102261. [CrossRef]
282. Mašek, O.; Buss, W.; Roy-Poirier, A.; Lowe, W.; Peters, C.; Brownsort, P.; Mignard, D.; Pritchard, C.; Sohi, S. Consistency of biochar properties over time and production scales: A characterisation of standard materials. *J. Anal. Appl. Pyrolysis* **2018**, *132*, 200–210. [CrossRef]
283. Musso, S.; Tulliani, J.-M.; Ferro, G.; Tagliaferro, A. Influence of carbon nanotubes structure on the mechanical behavior of cement composites. *Compos. Sci. Technol.* **2009**, *69*, 1985–1990. [CrossRef]
284. Gupta, S.; Kua, H.W. Carbonaceous micro-filler for cement: Effect of particle size and dosage of biochar on fresh and hardened properties of cement mortar. *Sci. Total Environ.* **2019**, *662*, 952–962. [CrossRef]
285. Mo, L.; Fang, J.; Huang, B.; Wang, A.; Deng, M. Combined effects of biochar and MgO expansive additive on the autogenous shrinkage, internal relative humidity and compressive strength of cement pastes. *Constr. Build. Mater.* **2019**, *229*, 116877. [CrossRef]
286. Muthukrishnan, S.; Gupta, S.; Kua, H.W. Application of rice husk biochar and thermally treated low silica rice husk ash to improve physical properties of cement mortar. *Theor. Appl. Fract. Mech.* **2019**, *104*, 102376. [CrossRef]
287. Gupta, S.; Kua, H.W. Effect of water entrainment by pre-soaked biochar particles on strength and permeability of cement mortar. *Constr. Build. Mater.* **2018**, *159*, 107–125. [CrossRef]
288. Dixit, A.; Gupta, S.; Pang, S.D.; Kua, H.W. Waste Valorisation using biochar for cement replacement and internal curing in ultra-high performance concrete. *J. Clean. Prod.* **2019**, *238*, 117876. [CrossRef]
289. Gupta, S.; Kua, H.W.; Pang, S.D. Effect of biochar on mechanical and permeability properties of concrete exposed to elevated temperature. *Constr. Build. Mater.* **2020**, *234*, 117338. [CrossRef]
290. Oancea, I.; Bujoreanu, C.; Budescu, M.; Benchea, M.; Grădinaru, C.M. Considerations on sound absorption coefficient of sustainable concrete with different waste replacements. *J. Clean. Prod.* **2018**, *203*, 301–312. [CrossRef]

291. Cuthbertson, D.; Berardi, U.; Briens, C.; Berruti, F. Biochar from residual biomass as a concrete filler for improved thermal and acoustic properties. *Biomass Bioenergy* **2019**, *120*, 77–83. [[CrossRef](#)]
292. Kua, H.W.; Gupta, S.; Aday, A.N.; Srubar, W.V. Biochar-immobilized bacteria and superabsorbent polymers enable self-healing of fiber-reinforced concrete after multiple damage cycles. *Cem. Concr. Compos.* **2019**, *100*, 35–52. [[CrossRef](#)]
293. Mu, B.; Wang, A. 11—Fabrication and Applications of Carbon/Clay Mineral Nanocomposites. In *Nanomaterials from Clay Minerals*; Wang, A., Wang, W., Eds.; Elsevier: Amsterdam, The Netherlands, 2019; pp. 537–587. [[CrossRef](#)]
294. Lee, H.; Yang, S.; Wi, S.; Kim, S. Thermal transfer behavior of biochar-natural inorganic clay composite for building envelope insulation. *Constr. Build. Mater.* **2019**, *223*, 668–678. [[CrossRef](#)]
295. Yang, S.; Wi, S.; Lee, J.; Lee, H.; Kim, S. Biochar-red clay composites for energy efficiency as eco-friendly building materials: Thermal and mechanical performance. *J. Hazard. Mater.* **2019**, *373*, 844–855. [[CrossRef](#)]
296. Dahal, R.K.; Acharya, B.; Saha, G.; Bissessur, R.; Dutta, A.; Farooque, A. Biochar as a filler in glassfiber reinforced composites: Experimental study of thermal and mechanical properties. *Compos. Part B Eng.* **2019**, *175*, 107169. [[CrossRef](#)]
297. Bartoli, M.; Rosi, L.; Frediani, M. Chapter 22—Synthesis and Applications of Unsaturated Polyester Composites. In *Unsaturated Polyester Resins*; Thomas, S., Hosur, M., Chirayil, C.J., Eds.; Elsevier: Amsterdam, The Netherlands, 2019; pp. 579–598. [[CrossRef](#)]
298. Rana, S.; Alagirusamy, R.; Joshi, M. A review on carbon epoxy nanocomposites. *J. Reinf. Plast. Compos.* **2009**, *28*, 461–487. [[CrossRef](#)]
299. Kim, S.; Pechar, T.W.; Marand, E. Poly (imide siloxane) and carbon nanotube mixed matrix membranes for gas separation. *Desalination* **2006**, *192*, 330–339. [[CrossRef](#)]
300. Khan, A.; Savi, P.; Quaranta, S.; Rovere, M.; Giorcelli, M.; Tagliaferro, A.; Rosso, C.; Jia, C. Low-cost carbon fillers to improve mechanical properties and conductivity of epoxy composites. *Polymers* **2017**, *9*, 642. [[CrossRef](#)] [[PubMed](#)]
301. Bartoli, M.; Giorcelli, M.; Rosso, C.; Rovere, M.; Jagdale, P.; Tagliaferro, A. Influence of Commercial Biochar Fillers on Brittleness/Ductility of Epoxy Resin Composites. *Appl. Sci.* **2019**, *9*, 3109. [[CrossRef](#)]
302. Giorcelli, M.; Khan, A.; Pugno, N.M.; Rosso, C.; Tagliaferro, A. Biochar as a cheap and environmental friendly filler able to improve polymer mechanical properties. *Biomass Bioenergy* **2019**, *120*, 219–223. [[CrossRef](#)]
303. Giorcelli, M.; Savi, P.; Khan, A.; Tagliaferro, A. Analysis of biochar with different pyrolysis temperatures used as filler in epoxy resin composites. *Biomass Bioenergy* **2019**, *122*, 466–471. [[CrossRef](#)]
304. Giorcelli, M.; Khan, A.; Tagliaferro, A.; Savi, P.; Berruti, F. Microwave characterization of polymer composite based on Biochar: A comparison of composite behaviour for Biochar and MWCNTs. In Proceedings of the 2016 IEEE International Nanoelectronics Conference (INEC), Chengdu, China, 9–11 May 2016; pp. 1–2.
305. Quaranta, S.; Savi, P.; Giorcelli, M.; Khan, A.A.; Tagliaferro, A.; Jia, C.Q. Biochar-polymer composites and thin films: Characterizations and applications. In Proceedings of the 2016 IEEE 2nd International Forum on Research and Technologies for Society and Industry Leveraging a better tomorrow (RTSI), Bologna, Italy, 7–9 September 2016; pp. 1–4.
306. Jagdale, P.; Koumoulos, E.P.; Cannavaro, I.; Khan, A.; Castellino, M.; Dragatogiannis, D.A.; Tagliaferro, A.; Charitidis, C.A. Towards green carbon fibre manufacturing from waste cotton: A microstructural and physical property investigation. *Manuf. Rev.* **2017**, *4*, 10. [[CrossRef](#)]
307. Khan, A.; Jagdale, P.; Castellino, M.; Rovere, M.; Jehangir, Q.; Mandracci, P.; Rosso, C.; Tagliaferro, A. Innovative functionalized carbon fibers from waste: How to enhance polymer composites properties. *Compos. Part B Eng.* **2018**, *139*, 31–39. [[CrossRef](#)]
308. Arrigo, R.; Jagdale, P.; Bartoli, M.; Tagliaferro, A.; Malucelli, G. Structure–Property Relationships in Polyethylene-Based Composites Filled with Biochar Derived from Waste Coffee Grounds. *Polymers* **2019**, *11*, 1336. [[CrossRef](#)]
309. Zhang, Q.; Khan, M.U.; Lin, X.; Cai, H.; Lei, H. Temperature varied biochar as a reinforcing filler for high-density polyethylene composites. *Compos. Part B Eng.* **2019**, *175*, 107151. [[CrossRef](#)]
310. Li, S.; Huang, A.; Chen, Y.-J.; Li, D.; Turng, L.-S. Highly filled biochar/ultra-high molecular weight polyethylene/linear low density polyethylene composites for high-performance electromagnetic interference shielding. *Compos. Part B Eng.* **2018**, *153*, 277–284. [[CrossRef](#)]

311. Bajwa, D.S.; Adhikari, S.; Shojaeiarani, J.; Bajwa, S.G.; Pandey, P.; Shanmugam, S.R. Characterization of bio-carbon and ligno-cellulosic fiber reinforced bio-composites with compatibilizer. *Constr. Build. Mater.* **2019**, *204*, 193–202. [[CrossRef](#)]
312. Das, O.; Bhattacharyya, D.; Sarmah, A.K. Sustainable eco-composites obtained from waste derived biochar: A consideration in performance properties, production costs, and environmental impact. *J. Clean. Prod.* **2016**, *129*, 159–168. [[CrossRef](#)]
313. Behazin, E.; Misra, M.; Mohanty, A.K. Sustainable biocarbon from pyrolyzed perennial grasses and their effects on impact modified polypropylene biocomposites. *Compos. Part B Eng.* **2017**, *118*, 116–124. [[CrossRef](#)]
314. Das, O.; Kim, N.K.; Kalamkarov, A.L.; Sarmah, A.K.; Bhattacharyya, D. Biochar to the rescue: Balancing the fire performance and mechanical properties of polypropylene composites. *Polym. Degrad. Stab.* **2017**, *144*, 485–496. [[CrossRef](#)]
315. Das, O.; Sarmah, A.K.; Bhattacharyya, D. Biocomposites from waste derived biochars: Mechanical, thermal, chemical, and morphological properties. *Waste Manag.* **2016**, *49*, 560–570. [[CrossRef](#)]
316. Das, O.; Bhattacharyya, D.; Hui, D.; Lau, K.-T. Mechanical and flammability characterisations of biochar/polypropylene biocomposites. *Compos. Part B Eng.* **2016**, *106*, 120–128. [[CrossRef](#)]
317. Das, O.; Sarmah, A.K.; Bhattacharyya, D. A sustainable and resilient approach through biochar addition in wood polymer composites. *Sci. Total Environ.* **2015**, *512*, 326–336. [[CrossRef](#)] [[PubMed](#)]
318. Poulouse, A.M.; Elnour, A.Y.; Anis, A.; Shaikh, H.; Al-Zahrani, S.M.; George, J.; Al-Wabel, M.I.; Usman, A.R.; Ok, Y.S.; Tsang, D.C.W.; et al. Date palm biochar-polymer composites: An investigation of electrical, mechanical, thermal and rheological characteristics. *Sci. Total Environ.* **2018**, *619*, 311–318. [[CrossRef](#)] [[PubMed](#)]
319. Nan, N.; DeVallance, D.B.; Xie, X.; Wang, J. The effect of bio-carbon addition on the electrical, mechanical, and thermal properties of polyvinyl alcohol/biochar composites. *J. Compos. Mater.* **2016**, *50*, 1161–1168. [[CrossRef](#)]
320. Nan, N.; DeVallance, D.B. Development of poly (vinyl alcohol)/wood-derived biochar composites for use in pressure sensor applications. *J. Mater. Sci.* **2017**, *52*, 8247–8257. [[CrossRef](#)]
321. Nan, W.; Zhao, Y.; Ding, Y.; Shende, A.R.; Fong, H.; Shende, R.V. Mechanically flexible electrospun carbon nanofiber mats derived from biochar and polyacrylonitrile. *Mater. Lett.* **2017**, *205*, 206–210. [[CrossRef](#)]
322. Ogunsona, E.O.; Misra, M.; Mohanty, A.K. Impact of interfacial adhesion on the microstructure and property variations of biocarbons reinforced nylon 6 biocomposites. *Compos. Part A Appl. Sci. Manuf.* **2017**, *98*, 32–44. [[CrossRef](#)]
323. Sheng, K.; Zhang, S.; Qian, S.; Fontanillo Lopez, C.A. High-toughness PLA/Bamboo cellulose nanowhiskers bionanocomposite strengthened with silylated ultrafine bamboo-char. *Compos. Part B Eng.* **2019**, *165*, 174–182. [[CrossRef](#)]
324. George, J.; Azad, L.B.; Poulouse, A.M.; An, Y.; Sarmah, A.K. Nano-mechanical behaviour of biochar-starch polymer composite: Investigation through advanced dynamic atomic force microscopy. *Compos. Part A Appl. Sci. Manuf.* **2019**, *124*, 105486. [[CrossRef](#)]
325. Das, O.; Hedenqvist, M.S.; Johansson, E.; Olsson, R.T.; Loho, T.A.; Capezza, A.J.; Singh Raman, R.K.; Holder, S. An all-gluten biocomposite: Comparisons with carbon black and pine char composites. *Compos. Part A Appl. Sci. Manuf.* **2019**, *120*, 42–48. [[CrossRef](#)]
326. Mardoyan, A.; Braun, P. Analysis of Czech subsidies for solid biofuels. *Int. J. Green Energy* **2015**, *12*, 405–408. [[CrossRef](#)]
327. Maroušek, J.; Hašková, S.; Zeman, R.; Váchal, J.; Vaníčková, R. Processing of residues from biogas plants for energy purposes. *Clean Technol. Environ. Policy* **2015**, *17*, 797–801. [[CrossRef](#)]
328. Lee, J.; Kim, K.-H.; Kwon, E.E. Biochar as a Catalyst. *Renew. Sustain. Energy Rev.* **2017**, *77*, 70–79. [[CrossRef](#)]
329. Lee, J.; Jung, J.-M.; Oh, J.-I.; Ok, Y.S.; Lee, S.-R.; Kwon, E.E. Evaluating the effectiveness of various biochars as porous media for biodiesel synthesis via pseudo-catalytic transesterification. *Bioresour. Technol.* **2017**, *231*, 59–64. [[CrossRef](#)]
330. Li, X.; Zhang, M.; Luo, J.; Zhang, S.; Yang, X.; Igalavithana, A.D.; Ok, Y.S.; Tsang, D.C.W.; Lin, C.S.K. Efficient succinic acid production using a biochar-treated textile waste hydrolysate in an in situ fibrous bed bioreactor. *Biochem. Eng. J.* **2019**, *149*, 107249. [[CrossRef](#)]

331. Delidovich, I.; Palkovits, R. Impacts of acidity and textural properties of oxidized carbon materials on their catalytic activity for hydrolysis of cellobiose. *Microporous Mesoporous Mater.* **2016**, *219*, 317–321. [[CrossRef](#)]
332. Kastner, J.R.; Miller, J.; Geller, D.P.; Locklin, J.; Keith, L.H.; Johnson, T. Catalytic esterification of fatty acids using solid acid catalysts generated from biochar and activated carbon. *Catal. Today* **2012**, *190*, 122–132. [[CrossRef](#)]
333. Zhong, Y.; Zhang, P.; Zhu, X.; Li, H.; Deng, Q.; Wang, J.; Zeng, Z.; Zou, J.-J.; Deng, S. Highly Efficient Alkylation Using Hydrophobic Sulfonic Acid-Functionalized Biochar as a Catalyst for Synthesis of High-Density Biofuels. *ACS Sustain. Chem. Eng.* **2019**, *7*, 14973–14981. [[CrossRef](#)]
334. Zhong, Y.; Deng, Q.; Zhang, P.; Wang, J.; Wang, R.; Zeng, Z.; Deng, S. Sulfonic acid functionalized hydrophobic mesoporous biochar: Design, preparation and acid-catalytic properties. *Fuel* **2019**, *240*, 270–277. [[CrossRef](#)]
335. Vidal, J.L.; Andrea, V.P.; MacQuarrie, S.L.; Kerton, F.M. Oxidized Biochar as a Simple, Renewable Catalyst for the Production of Cyclic Carbonates from Carbon Dioxide and Epoxides. *ChemCatChem* **2019**, *11*, 4089–4095. [[CrossRef](#)]
336. Areeprasert, C.; Khaobang, C. Pyrolysis and catalytic reforming of ABS/PC and PCB using biochar and e-waste char as alternative green catalysts for oil and metal recovery. *Fuel Process. Technol.* **2018**, *182*, 26–36. [[CrossRef](#)]
337. Yuan, Y.; Bolan, N.; PrévotEAU, A.; Vithanage, M.; Biswas, J.K.; Ok, Y.S.; Wang, H. Applications of biochar in redox-mediated reactions. *Bioresour. Technol.* **2017**, *246*, 271–281. [[CrossRef](#)]
338. Cao, X.; Huang, Y.; Tang, C.; Wang, J.; Jonson, D.; Fang, Y. Preliminary study on the electrocatalytic performance of an iron biochar catalyst prepared from iron-enriched plants. *J. Environ. Sci.* **2020**, *88*, 81–89. [[CrossRef](#)]
339. Noman, M.; Sanginario, A.; Jagdale, P.; Castellino, M.; Demarchi, D.; Tagliaferro, A. Pyrolyzed bamboo electrode for electrogenerated chemiluminescence of Ru (bpy) 32+. *Electrochim. Acta* **2014**, *133*, 169–173. [[CrossRef](#)]
340. Xiang, Y.; Liu, H.; Yang, J.; Shi, Z.; Tan, Y.; Jin, J.; Wang, R.; Zhang, S.; Wang, J. Biochar decorated with gold nanoparticles for electrochemical sensing application. *Electrochim. Acta* **2018**, *261*, 464–473. [[CrossRef](#)]
341. Ziegler, D.; Palmero, P.; Giorcelli, M.; Tagliaferro, A.; Tulliani, J.-M. Biochars as Innovative Humidity Sensing Materials. *Chemosensors* **2017**, *5*, 35. [[CrossRef](#)]
342. Jagdale, P.; Ziegler, D.; Rovere, M.; Tulliani, J.M.; Tagliaferro, A. Waste Coffee Ground Biochar: A Material for Humidity Sensors. *Sensors* **2019**, *19*, 801. [[CrossRef](#)] [[PubMed](#)]
343. Agustini, D.; Mangrich, A.S.; Bergamini, M.F.; Marcolino-Junior, L.H. Sensitive voltammetric determination of lead released from ceramic dishes by using of bismuth nanostructures anchored on biochar. *Talanta* **2015**, *142*, 221–227. [[CrossRef](#)] [[PubMed](#)]
344. Oliveira, P.R.; Lamy-Mendes, A.C.; Rezende, E.I.P.; Mangrich, A.S.; Marcolino Junior, L.H.; Bergamini, M.F. Electrochemical determination of copper ions in spirit drinks using carbon paste electrode modified with biochar. *Food Chem.* **2015**, *171*, 426–431. [[CrossRef](#)] [[PubMed](#)]
345. Oliveira, P.R.d.; Lamy-Mendes, A.C.; Gogola, J.L.; Mangrich, A.S.; Marcolino Junior, L.H.; Bergamini, M.F. Mercury nanodroplets supported at biochar for electrochemical determination of zinc ions using a carbon paste electrode. *Electrochim. Acta* **2015**, *151*, 525–530. [[CrossRef](#)]
346. Oliveira, P.R.; Kalinke, C.; Mangrich, A.S.; Marcolino-Junior, L.H.; Bergamini, M.F. Copper hexacyanoferrate nanoparticles supported on biochar for amperometric determination of isoniazid. *Electrochim. Acta* **2018**, *285*, 373–380. [[CrossRef](#)]
347. de Oliveira, P.R.; Kalinke, C.; Gogola, J.L.; Mangrich, A.S.; Junior, L.H.M.; Bergamini, M.F. The use of activated biochar for development of a sensitive electrochemical sensor for determination of methyl parathion. *J. Electroanal. Chem.* **2017**, *799*, 602–608. [[CrossRef](#)]
348. Kalinke, C.; Wosgrau, V.; Oliveira, P.R.; Oliveira, G.A.; Martins, G.; Mangrich, A.S.; Bergamini, M.F.; Marcolino-Junior, L.H. Green method for glucose determination using microfluidic device with a non-enzymatic sensor based on nickel oxyhydroxide supported at activated biochar. *Talanta* **2019**, *200*, 518–525. [[CrossRef](#)]
349. Martins, G.; Gogola, J.L.; Caetano, F.R.; Kalinke, C.; Jorge, T.R.; Santos, C.N.D.; Bergamini, M.F.; Marcolino-Junior, L.H. Quick electrochemical immunoassay for hantavirus detection based on biochar platform. *Talanta* **2019**, *204*, 163–171. [[CrossRef](#)]

350. Huang, J.-F.; Shi, Q.-S.; Feng, J.; Chen, M.-J.; Li, W.-R.; Li, L.-Q. Facile pyrolysis preparation of rosin-derived biochar for supporting silver nanoparticles with antibacterial activity. *Compos. Sci. Technol.* **2017**, *145*, 89–95. [[CrossRef](#)]
351. Bock, E.M.; Coleman, B.S.L.; Easton, Z.M. Effect of biochar, hydraulic residence time, and nutrient loading on greenhouse gas emission in laboratory-scale denitrifying bioreactors. *Ecol. Eng.* **2018**, *120*, 375–383. [[CrossRef](#)]
352. Duan, X.; Chen, Y.; Yan, Y.; Feng, L.; Chen, Y.; Zhou, Q. New method for algae comprehensive utilization: Algae-derived biochar enhances algae anaerobic fermentation for short-chain fatty acids production. *Bioresour. Technol.* **2019**, *289*, 121637. [[CrossRef](#)] [[PubMed](#)]



© 2020 by the authors. Licensee MDPI, Basel, Switzerland. This article is an open access article distributed under the terms and conditions of the Creative Commons Attribution (CC BY) license (<http://creativecommons.org/licenses/by/4.0/>).